Blowing in the Wind: I. Velocities of Chondrule-sized Particles in a Turbulent Protoplanetary Nebula

Jeffrey N. Cuzzi[1] and Robert C. Hogan[2]
[1] Space Science Division, Ames Research Center; cuzzi@cosmic.arc.nasa.gov
[2] Bay Area Environmental Research, inc.; hogan@cosmic.arc.nasa.gov
Submitted to Icarus, September 17, 2002

Abstract: Small but macroscopic particles - chondrules, higher temperature mineral inclusions, metal grains, and their like - dominate the fabric of primitive meteorites. The properties of these constituents, and their relationship to the fine dust grains which surround them, suggest that they led an extended existence in a gaseous protoplanetary nebula prior to their incorporation into their parent primitive bodies. In this paper we explore in some detail the velocities acquired by such particles in a turbulent nebula. We treat velocities in inertial space (relevant to diffusion), velocities relative to the gas and entrained microscopic dust (relevant to accretion of dust rims), and velocities relative to each other (relevant to collisions). We extend previous work by presenting explicit, closed-form solutions for the magnitude and size dependence of these velocities in this important particle size regime, and compare these expressions with new numerical calculations. The magnitude and size dependence of these velocities have immediate applications to chondrule and CAI rimming by fine dust, and to their diffusion in the nebula, which we explore separately.

1 Background

The fabric of the most primitive meteorites undoubtedly contains many clues as to their origin. While most chondrites are samples of surfaces that have been well worked over by impacts and stirring ("regolith breccias"), the dominance of chondrules and like-sized objects remains clear. How it came about that most chondrite parent bodies are so dominated by particles with such a well-defined range of physical, chemical, and petrographic properties remains one of the big puzzles of meteoritics. Since there are relatively few examples of anything larger than 0.1-10 mm size particles in most primitive planetesimals, the way such particles interact with the gaseous nebula is of prime importance.

Fe-Mg-Si-O mineral chondrules, which solidified from a melt, constitute 30-80% of primitive meteorites. There are a number of extant hypotheses for the formation of the chondrules. Most workers in the field believe that chondrules are formed by either localized or nebula scale energetic events operating on freely floating precursors of comparable mass, at some location or locations in the protoplanetary nebula. However, some still maintain they are made in or on primitive bodies, or in collisions between them. In a hybrid scenario, some suggest they are formed in shock waves generated by already-formed planetesimals, and thus that they are a secondary phenomenon to primary accretion of planetesimals. See *eg.* Grossman (1989), Grossman *et al.* (1989), Boss (1996), Connolly and Love (1999), and Jones *et al.* (2000) for reviews of hypotheses on this long-controversial and perennially fascinating subject.

Another meteorite constituent of great interest are the mineral grains called Ca-Al-rich refractory inclusions (CAIs) - so called because their constituent minerals condense out of nebula gas at a much higher temperature than do chondrules. These objects are widely believed to be direct nebula condensates, and have a complex subsequent thermal history which has some similarities to that of chondrules and some differences. There is some indication from radioisotope ages that CAIs might be $\sim 10^6$ years older than the chondrules, but this remains slightly controversial. They make up 1-10% of primitive meteorites depending on type, and their size distribution is broader than that of the chondrules. How these high-temperature minerals find themselves intimately mixed with lower-temperature minerals remains a puzzle.

It remains unresolved at this time whether the nebula gas was turbulent or laminar during the chondrule era. In previous papers, we have suggested that some of the observed properties of chondrules themselves - their typical size and size distribution - can be associated with, and easily explained by, the effects of weak nebula turbulence (Cuzzi et al 1996, 2001). Nevertheless, a consistent end-to-end scenario for *formation* of primitive bodies in this environment, and relying on these processes, is not yet in hand. In this paper, we focus on the velocity evolution of this specific class of particles in a weakly turbulent nebula as a step towards developing a more complete scenario that operates to produce primitive bodies in a similar way across a variety of environments. The velocity evolution is critical for our understanding of several important aspects of chondrules and chondrites: (a) the radial distribution and redistribution or transport of chondrules and/or CAIs, once formed, before their accumulation into parent bodies; (b) The presence of fine grained rims on chondrules, CAIs, and other coarse particles in primitive chondrites (Metzler and Bischoff 1996, Brearley and Jones 1998); and (c) collision rates and velocities between chondrule-sized particles. The main goal of this paper is to provide a theoretical framework within which we can better understand mm-to-cm-size particle evolution in general. We accomplish this in sections 1 (analytical theory) and 2 (supporting numerical calculations). In another paper we apply these results to diffusion and dust rimming (Cuzzi 2002b).

1.1 Particle Velocities in Turbulence

Astrophysical modeling of the basic physics of particle behavior in fluid flows, laminar or turbulent, tends to begin and end with the classic papers by Whipple (1973), Adachi *et al.* (1976), Weidenschilling (1977, 1980), and Völk *et al.* (1980, henceforth VJMR; also Völk *et al.* 1978), with important recent updates by Markiewicz *et al.* (1991; henceforth MMV). In the fluid dynamics literature, however, the study of particle motions in fluid flows has both a long history, and a robust ongoing presence. This history is nicely summarized by Meek and Jones (1973). More recent work in the fluids literature is noted in various relevant places below. VJMR first developed a useful formalism for calculating the dispersion velocities V_p (relative to inertial space) and collision velocities V_{pp} (relative to each other) of particles in a turbulent nebula. They circumvented the thorny problem of "essential nonlinearity" (*cf.* Meek and Jones 1973) by translating clever physical insights into mathematics and adopting a velocity autocorrelation function approach, which we discuss in more detail below. While it serves an important internal role in their solutions, neither VJMR nor MMV say much about the relative velocity between particles and gas, V_{pg}. Yet, V_{pg} is the determinant quantity for

accretion of rims of fine dust grains by small, macroscopic objects (Paque and Cuzzi 1997, Cuzzi et al 1998, Morfill *et al.* 1998). Our goal in this paper is to quantify V_p, V_{pg}, and V_{pp} for such particles in a way that extends and focusses the formulation of VJMR and MMV, and which allows insights to be gained into the history of chondrules and like-sized particles in the protoplanetary nebula.

In this paper, we determine velocities of all three kinds - V_p, V_{pg}, and V_{pp} - with emphasis on particles having stopping times t_s comparable to the overturn time t_η of Kolmogorov scale eddies. Particles in this size regime have behavior more complex than tiny "dust" grains, which are essentially trapped to the gas flow on all scales. In particular, particles with $t_s = t_\eta$ are subject to "preferential concentration" by large factors in turbulence, and based on some of its apparent fingerprints in the meteorite record, we have suggested a link between this process, chondrules, and primary accretion. Specifically, we refer to the fact that the *typical size* and the *shape of the size distribution* of chondrules are readily explained by turbulent concentration (Cuzzi et al 1996, 2001). In a parallel paper (Cuzzi 2002b) we explore the possibility that the functional form of V_{pg} might reveal another fingerprint of turbulent concentration, and that turbulence might help us understand the puzzling mix of CAIs and chondrules in the same meteorites.

Particles are aerodynamically classified by their Stokes number St, the ratio of their stopping time t_s to the overturn time of some characteristic eddy. We will make use of Stokes numbers defined relative to two different eddy overturn timescales: the Stokes number relative to the largest, or integral scale eddy time t_L: $St_L = t_s/t_L$, and that defined relative to the smallest, or Kolmogorov scale eddy time t_η: $St_\eta = t_s/t_\eta$. The overturn time of the largest scale eddy t_L is generally regarded as the local orbit period. Preferentially concentrated particles (chondrules, we believe) have $St_\eta = 1$ and $St_L \lesssim\!< 1$. For these particles, which are smaller than the gas molecular mean free path, the stopping time $t_s = r\rho_s/c\rho_g$, where r is particle radius, ρ_s is particle material density, c is the nebula sound speed, and ρ_g is the nebula gas density (Weidenschilling 1977). That is, t_s and thus both St_L and St_η are *linearly proportional to particle radius.*

1.2 Previous work; the autocorrelation function

We briefly review and simplify the notation of VJMR and MMV. VJMR assumed a fully developed inertial range of turbulence with some largest, or integral scale L and zero smallest scale. MMV also adopted the Kolmogorov energy spectrum (as shall we) but correctly pointed out that turbulence ceases for scales smaller than the Kolmogorov or inner scale η. Especially for small particles in the chondrule-and-CAI size range, MMV point out that this has important implications for V_p and V_{pp}, and we will show that the implications are important for V_{pg} as well. In a Kolmogorov spectrum, an inertial range of turbulent gas kinetic energy extends from the largest or integral scale $l = L$ to the smallest or Kolmogorov scale $l = \eta$. Following VJMR, we work in the spatial frequency regime, where $k(l) = 2\pi/l$ and $E(k) = E_L(k/k_L)^{-5/3}$ for the Kolmogorov spectrum (note our $E(k)$ is a true energy, and is half of VJMR's $P(k)$). Then $v(k) = (2kE(k))^{1/2}$ and $t(k) = 1/(kv(k)) = t_L(k/k_L)^{-2/3}$. As did MMV, we assume $E(k) = 0$ for $k > k_\eta$ (no turbulent energy at scales smaller than the Kolmogorov scale). The mean square turbulent (fluctuating) gas velocity is V_g; thus the typical turbulent kinetic energy per unit gas mass is $V_g^2/2$, providing the normalization

criterion:

$$\int_{k_L}^{k_\eta} E(k)dk = V_g^2/2 = \int_{k_L}^{k_\eta} E_L(k/k_L)^{-5/3}dk = \frac{3}{2}E_L k_L. \quad (1)$$

The turbulent gas motions induce fluctuating velocities in the particle population, leading to diffusion (V_p), mutual collisions (V_{pp}), and motion relative to the local gas (V_{pg}).

VJMR derive V_p formally by a backwards time integration of the instantaneous acceleration (their equations 5 and 6):

$$V_p(t) = t_s^{-1} \int_0^t \exp\left(-(t-t')/t_s\right) V_g(t')dt' \quad (2)$$

where $V_g(t')$ represents the fluctuating gas velocity history along a particle trajectory (formally unknown at this point). They proceed by approximating $V_g(t')$ as an integral over all (independently acting) spatial frequencies k with eddy timescales t_k, and approximate the contributions as coming from two classes of eddies: "class 1" eddies, with overturn times long enough ($t_k > t_s$) that particles are always in equilibrium within them, and are primarily just advected by their (temporally fluctuating) motions, and "class 3" eddies with overturn times too short ($t_k < t_s$) for the particle to come to equilibrium as it passes through them. Intermediate, or what might be "class 2" eddies are not treated separately, but simply absorbed into the classes on either side. Different simplifications are allowed for each class. The boundary between eddy classes 1 and 3 is k^*, where $t_{k*} = t_s$. VJMR show that the class 3 (small, fast) eddies are negligible for velocity components V_p and V_{pg}, but dominate the contributions to V_{pp}. We will make use of these results below.

VJMR first obtain the product $< V_p(t)V_p(t) >=< V_p^2 >$ by integrating backwards over two separate time histories. They introduce the gas velocity autocorrelation function for gas velocities (in their equation 16) $R(t,t';k) = \exp\left(-|t-t'|/t_k\right)$. While they don't make the distinction, the autocorrelation function to be used in this way is properly that determined *along a particle trajectory* (Batchelor 1948, Hinze 1975, Squires and Eaton 1990, Elghobashi 1991), and is thus a function of t_s in general. However, for $St_L << 1$, and at this stage of our knowledge, this distinction is not significant (Squires 1990).

Subsequently, MMV suggested a more general, even if *ad hoc*, functional form for $R(t,t';k)$:

$$R(t,t';k) = \left(1 + \frac{|t-t'|}{t_k}\right)^n e^{(-|t-t'|/t_k)}, \quad (3)$$

with $n = 0$ or 1. They note that the $n = 1$ case has more plausible physical behavior (zero slope) near $t = t'$ than the $n = 0$ (pure exponential) form assumed by VJMR.

1.2.1 New results regarding the form of the autocorrelation function, and the value of n:

The selection of $n = (0, 1)$ determines the form of the fluid velocity autocorrelation function $R(t,t';k)$. Squires (1990) measured this function directly in his direct numerical simulations of turbulence, by following fluid motions along the trajectories of a number of particles with different St_L. In **figure 1** we compare the results of Squires (1990) with the predictions based on the $n = 0$ and $n = 1$ expressions of MMV for $R(t,t';k)$. Note that, since MMV

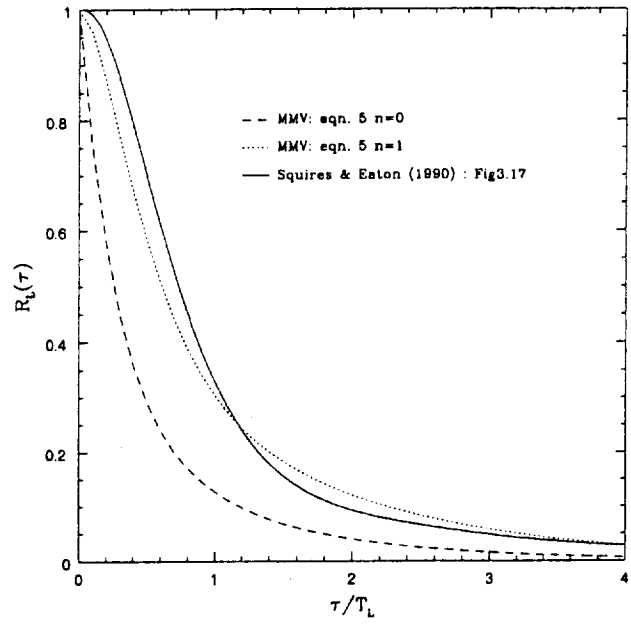

Figure 1: Autocorrelation function for gas velocities along the trajectory of a $St_\eta = 1$ particle, as computed directly from our simulations (dotted) and from the simulations of Squires (1990), and as calculated using the $n = 0$ and $n = 1$ models of MMV. Here, $\tau = t - t'$ and is normalized by the large eddy turnover time T_L. The $n = 1$ model is clearly the better choice.

express their autocorrelation function as a function of k, it must be integrated over an energy spectrum to compare with the numerical results of Squires (1990). Because Squires (1990) only calculated a 1-D autocorrelation function (*ie.*, using only one velocity component), we integrated the $R(t, t'; k)$ of MMV over a 1D energy spectrum (essentially, one-third of the total $E(k)$) (see also Squires and Eaton 1991). It is clear from figure 1 that $n = 1$ is the better choice. This has important implications, primarily for V_{pg} and V_{pp}. In section 2, we directly compare V_p and V_{pg} calculated in full 3D turbulence using the two alternate autocorrelation functions, and again reach the same conclusion.

1.3 Particle random velocities relative to inertial space

After some algebra, VJMR derive an expression (their equation 18) for the mean square particle fluctuating velocity V_p, of which we need only the large, slow (class 1) eddy contribution since the small eddy contribution is negligible for $St_\eta = 1$ particles (we will henceforth drop the $<>$ notation on V_p, V_g, V_{pg}, and V_{pp}, and will merely recall that all are statistical expectation values based on extensive temporal or spatial averaging). Because of our emphasis on particles with $St_\eta = 1$, we also replace the upper limit of VJMR's class 1 integral (k^*) with the Kolmogorov scale k_η. This simplification is, in fact, actually fairly good over the entire range of $St_L << 1$, *precisely because* the contribution of eddies on smaller scales than k^* (the class 3 eddies) is negligible. That is, the upper limit can be extended from k^* to k_η *in general* for mathematical simplicity without incurring significant error. Mathematically,

the upper limit could even be extended to infinity (*eg.*, Völk *et al.* 1980), but the important role of the Reynolds number and of the Kolmogorov scale is then lost. Thus,

$$V_p^2 \approx 2 \int_{k_L}^{k_\eta} E(k) \frac{t_k}{t_k + t_s} dk. \tag{4}$$

Similarly, the generalized MMV expression for V_p^2 (their equation 6) can be simplified to

$$V_p^2 \approx 2 \int_{k_L}^{k_\eta} E(k) \left(1 - \left(\frac{t_s}{t_k + t_s}\right)^{n+1}\right) dk = 2 \int_{k_L}^{k_\eta} E(k) \left(1 - \left(\frac{1}{1 + t_k/t_s}\right)^{n+1}\right) dk \tag{5}$$

for the particle size regime of interest here. As did VJMR, MMV note that the second integral of their equation (6) - the class 3 eddy contribution - is negligible for small particles, so we retain only the first integral of their equation (6). We again simplify the upper limit of integration in the remaining integral for the nominal $St_\eta \approx 1$ case where $k^* \approx k_\eta >> k_L$. We validate this by comparing our results with those of MMV (section 1.7).

The result for V_p^2 was plotted, but not stated explicitly, by VJMR and MMV (figure 1 in both papers), and explicitly derived by Cuzzi *et al.* (1993; Appendix B): $V_p^2 = V_g^2/(1+St_L)$. It is simple to see why $V_p^2 \approx V_g^2$ in the limit $St_L << 1$ and certainly for $St_\eta \approx 1$, since $t_s << t_k$ in equations (4) or (5) for nearly all k and overwhelmingly all $E(k)$. This limit is appropriate for chondrule-and-CAI-sized particles even in the presence of their small vertical settling velocity - they diffuse nearly as well as a gas molecule, and do not "settle to the midplane" in even a very weakly turbulent nebula (Dubrulle *et al.* 1995, Cuzzi *et al.* 1996). The implications are discussed in section 3. However, V_p^2 and V_g^2 are not *exactly* equal, resulting in a small, but very important, relative energy of motion V_{pg}^2, giving the velocity with which particles move through the gas and encounter tiny (micron-sized) dust grains.

1.4 Particle velocities relative to the gas

The average relative velocity magnitude between a particle and the turbulent gas is V_{pg}. VJMR make use only of the spatial frequency components of this quantity, which they refer to as $V_{rel}(k)$ (their equation 15). Practically speaking, however, a particle will instantaneously sense all eddy contributions as one V_{pg}; we obtain this by merely integrating VJMR equation (15) over k. Considering only the part of the expression relevant for $St_\eta \approx 1$ (that for $k^* > k_L$), neglecting any systematic velocity, and again letting $k^* \approx k_\eta >> k_L$, the second integral vanishes and we obtain

$$V_{pg}^2 \approx 2 \int_{k_L}^{k_\eta} E(k) \left(\frac{t_s}{t_k + t_s}\right) dk. \tag{6}$$

For this $n = 0$ case treated by VJMR, it can be easily verified using equations (4) and (6) that

$$V_{pg}^2 + V_p^2 = 2 \int_{k_L}^{k_\eta} E(k) dk = V_g^2. \tag{7}$$

However, this useful result is true independent of n. It may also be obtained by Fourier transform solution of the forcing equations in temporal frequency (ω) space, where the

energy spectrum of gas velocity fluctuations $E_g(\omega)$, particle velocity fluctuations $E_p(\omega)$, and relative velocity fluctuations $E_{pg}(\omega)$ are related by

$$E_p(\omega) = E_g(\omega)/(1 + t_s^2\omega^2) \quad \text{and} \quad E_{pg}(\omega) = t_s^2\omega^2 E_p(\omega). \tag{8}$$

This approach can be traced to Csanady (1963); it is also described by Hinze (1975, chapter 5), Meek and Jones (1973), and Squires (1990, sections 4.2 and 4.5.1)). The E_p solution was also derived in this way by Cuzzi *et al.* (1993, Appendix B). It is also clear then that $E_{pg}(\omega) + E_p(\omega) = E_g(\omega)$, essentially the same result as equation (7) above. Finally, we have directly verified equation (7) in our numerical simulations.

Using this general relationship, we can extend the results of MMV to obtain V_{pg}^2 for their more generalized gas velocity autocorrelation functions (they only present results for V_p^2). That is, using equations (1) and (5),

$$V_{pg}^2 = V_g^2 - V_p^2 = 2\int_{k_L}^{k_\eta} E(k)(\frac{t_s}{t_s + t_k})^{n+1} dk = 2\int_{k_L}^{k_\eta} E(k)\left(\frac{1}{1 + t_k/t_s}\right)^{n+1} dk. \tag{9}$$

We will use equations (5) and (9), with assumed inertial range expressions for $E(k)$, to derive analytical expressions for V_p and V_{pg} of hypothetically "chondrule-like" (*ie.*, $St_\eta \approx 1$) particles as functions of their size and the turbulent Reynolds number.

1.5 Relative velocities between particles of similar sizes

Expressions for V_{pp} (VJMR Appendix C and equation 19; MMV equations 7 and 8) are more cumbersome, but respond nicely to certain simplifying assumptions. The full expression for V_{pp} for two particles of equal size is (changing notation slightly from MMV equation 9, and allowing for a finite Kolmogorov scale):

$$V_{pp}^2 = 4\int_{k^*}^{k_\eta} E(k)\left(1 - \frac{t_s}{t_s + t_k}\right)\left[g(\chi) + \frac{nt_s h(\chi)}{t_s + t_k}\right] dk, \tag{10}$$

where $g(\chi) = \tan^{-1}(\chi)/\chi$ and $h(\chi) = 1/(1 + \chi^2)$. The parameter χ of VJMR and MMV is small in our regime of interest:

$$\chi = \frac{V_{rel}(k)t_s(kt_k)}{t_s + t_k} = \frac{V_{rel}(k)t_s}{v(k)(t_s + t_k)} \approx \frac{V_{rel}(k)}{2v(k)} < 1, \tag{11}$$

since in the very limited range of k over which the integral is done, $t_s \approx t_k$.[1] In fact $\chi << 1$ over most of the integral where $t_s << t_k$, so the functions $g(\chi)$ and $h(\chi)$ are ≈ 1 or perhaps as small as a fraction of order unity; thus

$$V_{pp}^2 \approx 4\int_{k^*}^{k_\eta} E(k)\left[1 - \left(\frac{t_s}{t_s + t_k}\right)^{n+1}\right] dk = 4\int_{k^*}^{k_\eta} E(k)\left[1 - \left(\frac{1}{1 + t_k/t_s}\right)^{n+1}\right] dk. \tag{12}$$

The integrand is identical to that for V_p^2, but the integral has different limits which make it clear that only the eddies faster than t_s can perturb identical particles into having incoherent relative velocities.

[1] In the above equation, the mathematical generalization of V_{pg} by VJMR and MMV to its $k-$th components $V_{rel}(k)$ momentarily reappears. However, it is true in general, at any spatial frequency, that the particle-gas relative velocity is less than, or at most equal to, the gas velocity itself.

1.6 Scaling relations

Recall that for the gas,

$$t_k = l(k)/v(k) = (L/V_g)(k/k_L)^{-2/3} = t_L(k/k_L)^{-2/3} \tag{13}$$

(Cuzzi *et al.* 2001). In equation (13) we have made the usual identification of V_g with the largest scale eddy L. For the particles,

$$\frac{t_s}{t_L} = St_L = (k_s/k_L)^{-2/3} \tag{14}$$

and

$$\frac{t_s}{t_k} = (k/k_s)^{2/3} = \frac{t_s}{t_L}(k/k_L)^{2/3} = St_L(k/k_L)^{2/3}, \tag{15}$$

Note that if we restrict our attention to particles *with* $St_\eta = t_s/t_\eta \approx 1$, then their Stokes number referred to the *integral* scale automatically becomes

$$St_L = t_s/t_L = t_\eta/t_L = (k_\eta/k_L)^{-2/3} = (Re^{3/4})^{-2/3} = Re^{-1/2}. \tag{16}$$

The last substitution of $(k_\eta/k_L) = Re^{3/4}$, where $Re = LV_g/\nu$ is the flow Reynolds number, with ν being the molecular kinematic viscosity, is a direct consequence of the definitions of the Kolmogorov scale, the energy dissipation rate, and the Reynolds number (Tennekes and Lumley 1972). This relation can be obtained without any reference at all to the Kolmogorov spectrum but merely using scaling arguments relating to t_L and t_η.[2] Re is related to astrophysical "α"-models of the protoplanetary nebula by $Re = \alpha cH/\nu$ with c = sound speed and H = nebula vertical scale height (Cuzzi *et al.* 2001).

1.7 Final expressions for V_{pg} and V_{pp}

Substituting the scaling relations from above for t_s/t_k, equation (9) for V_{pg} becomes

$$V_{pg}^2 = 2\int_{k_L}^{k_\eta} E(k)\left(\frac{1}{1+t_k/t_s}\right)^{n+1} dk = 2\int_{k_L}^{k_\eta} E(k)\left(\frac{St_L}{St_L+(k/k_L)^{-2/3}}\right)^{n+1} dk. \tag{17}$$

We use the normalization (equation 1) to write $E(k) = (V_g^2/3k_L)(k/k_L)^{-5/3}$, and change integration variable to $x = k/k_L$, leaving

$$V_{pg}^2 = \frac{2V_g^2}{3}\int_1^{Re^{3/4}} \left(\frac{St_L}{St_L+x^{-2/3}}\right)^{n+1} x^{-5/3}dx. \tag{18}$$

where in the upper limit we have substituted $k_\eta/k_L = Re^{3/4}$ from the scaling relations. Closed form solutions for equation (18) can be obtained for $n = 0$ or 1. For example, for $n = 1$ the result of the integral is

$$V_{pg}^2 = V_g^2\left[\frac{St_L}{1+St_Lx^{2/3}}\right]_{Re^{3/4}}^1 = V_g^2\left[\frac{St_L^2(Re^{1/2}-1)}{(St_L+1)(St_LRe^{1/2}+1)}\right]. \tag{19}$$

[2]Let the energy dissipation rate be ϵ. Then $\epsilon = V_g^2/t_L = V_g^3/L$ where the first expression defines t_L and the last expression defines L. Also $t_\eta = (\nu/\epsilon)^{1/2}$ and $\eta = (\nu^3/\epsilon)^{1/4}$. Solving gives $t_L/t_\eta = Re^{1/2}$ and $\eta/L = Re^{3/4}$.

For $n = 0$ the result of the integral is:

$$V_{pg}^2 = V_g^2 \left[St_L \ln \left(\frac{Re^{1/2}(1 + St_L)}{Re^{1/2} St_L + 1} \right) \right]. \tag{20}$$

These results make it quite easy to predict both the magnitude and the St_η dependence of V_{pg} for arbitrary nebula turbulent intensity.

We solve equation (12) for V_{pp} in a similar fashion to the solution for V_{pg} above, to obtain for $n = 1$:

$$V_{pp}^2 = \frac{4V_g^2}{3} \int_{k(t_s)/k_L}^{k_\eta/k_L} \left(\frac{2St_L x^{-7/3} + x^{-9/3}}{St_L^2 + 2St_L x^{-2/3} + x^{-4/3}} \right) dx. \tag{21}$$

As before, the upper integration limit is $k_\eta/k_L = Re^{3/4}$. For the lower limit, $k^*/k_L = k(t_s)/k_L = (t_s/t_L)^{-3/2} = St_L^{-3/2}$ from the scaling relations. The closed form analytic solution of this integral is:

$$V_{pp}^2 = 2V_g^2 \left[\frac{x^{-2/3}}{1 + St_L x^{2/3}} \right]_{Re^{3/4}}^{St_L^{-3/2}} = 2V_g^2 \left[\frac{St_L}{2} - \frac{1}{St_L Re + Re^{1/2}} \right]. \tag{22}$$

The $n = 0$ form of the solution is somewhat less useful, and we note it without expanding it as it will not be used further.

$$V_{pp}^2 = 2V_g^2 \left[St_L \ln \left(\frac{1 + St_L x^{2/3}}{x^{2/3}} \right) - \frac{1}{x^{2/3}} \right]_{St_L^{-3/2}}^{Re^{3/4}}.$$

1.8 Detailed comparisons with the models of Markiewicz *et al.*

In addition to developing the analytical expressions discussed and applied in the paper, we also developed a detailed numerical model following the prescriptions of MMV exactly (but with a generalized turbulent energy spectrum). This was needed both to evaluate their theoretical approach in the context of our numerical simulations of turbulence (section 2), which have a non-Kolmogorov spectrum and low Reynolds number compared to nebula applications, and to assess the validity of our analytical approximations. The numerical model of MMV is no longer in active use (W. Markiewicz, personal communication 2002), so we digitized their V_{pp} results (their figure 5) to facilitate comparisons. As seen in **figure 4**, our full numerical model for V_{pp} (solid curves) agrees very well with their results for V_{pp} (long dashed curves). In figure 2 we also show our results for V_{pg}, not presented by VJMR or MMV, as obtained by integrating MMV equation 4 over all spatial frequencies. Note that we, and MMV, both use the appropriate form of $R(t, t'; k)$ (*ie.*, that for the correct choice of n; section 1.2) for these calculations.

The most striking feature of the results, first noted by MMV, is that V_{pp} very quickly falls to zero for particles with $St_\eta < 1$ (*i.e.* $St_L < Re^{-1/2}$, as shown in the scaling relations of section 1.6 above) because there is no more energy in faster eddies to provide relative velocities to such particles. This does not happen to V_{pg}, because eddies on all scales contribute. Also note that V_p and V_{pp} decrease for *large* particles ($St_L > 1$), as fewer eddies can effectively

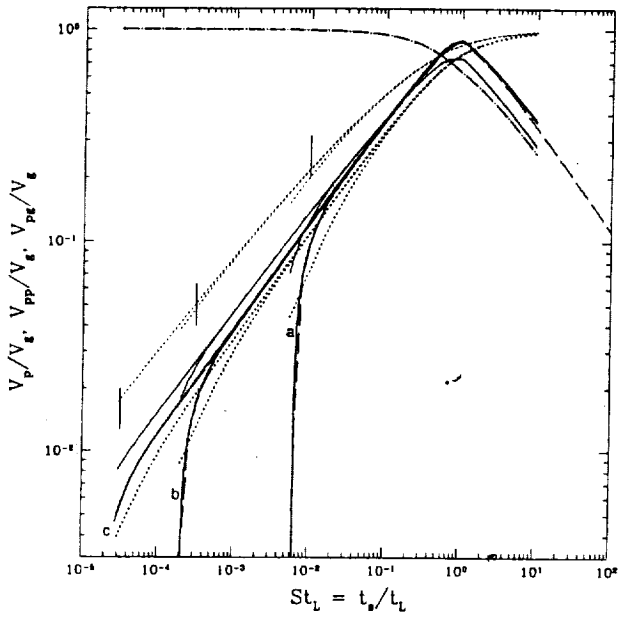

Figure 2: Comparison of our numerical version of the full MMV model for $n = 0$ (light curves) and $n = 1$ (heavy curves), along with digitized results for V_{pp} from MMV (dashed curves, their figure 5, for $n = 1$). Three different Re are shown: (a) 10^4, (b) 10^7, and (c) 10^9. The dash-dot curves are for V_p, which has the same shape for all three Re. V_{pg} is shown in the two sets of dotted curves and V_{pp} in the two sets of solid curves. Note that the $n = 0$ values of V_{pg} (light dotted curves) are considerably (3-4 times) higher than the preferred $n = 1$ values (heavy dotted curves), *and* the St_L-dependence of V_{pg}, for $n = 0$, never gets much above 0.5, whereas for $n = 1$ a linear dependence is seen for $St_L < Re^{-1/2}$. As in figures 4 and 5, vertical hash marks correspond to $St_L = Re^{-1/2}$ for the three values of Re.

couple to particles with such long stopping times. Naturally, V_{pg} simply approaches V_g for these large particles.

Upon comparing our original analytical results (equations 19 and 22) with our full numerical model and the MMV results, we found some small quantitative discrepancies at the order unity level, as might be expected. The responsible approximations were easily identified. First, we approximated the boundary between class 1 and class 3 eddies by $t_s = t(k^*)$ rather than the more complete equation 9 of VJMR and equation 4 of MMV, which obtains the relevant eddy frequency in the moving frame of the particle and involves $V_{rel}(k)$. Comparison of the two criteria revealed that, to a very good approximation, the criterion $t_s = t(k^*)$ gives a value of k^* that is too large by a factor close to 2 (**figure 3**). So, after this "calibration", we merely decrease the lower limit of integration in our equation (22) by a factor of 2. Second, even after this correction, our values of V_{pp} are about 20% high. This is easily ascribed to our approximation that $g(\chi)$ and $h(\chi)$ are equal to unity throughout the entire range of k; in fact, they are tens of percent smaller than unity over some part of this range, depending on the value of St_L. Empirically, this is corrected by multiplying our analytical expression for V_{pp} by a constant factor of 0.8. With these two simple adjustments, each correcting a known oversimplification, our analytical expression for V_{pp} achieves very good good agreement with the MMV results, and with our own full numerical model, over the relevant range of $St_L \leq 0.1$ or so. There appears to be no reason to make such refinements to our analytical expression for V_{pg} (equatión 19), because our approximations are better justified and the agreement with MMV acceptable.

1.9 Numerical refinements to the model

With insights gained from comparison of our numerical and analytical models, we have made two small adjustments to equation (22) for V_{pp} which correct for two of our approximations. Equation (22) is multiplied by a factor of 0.8, and the upper integration limit ($St_L^{-3/2}$) is divided by two, so the first term in the final expression changes from $St_L/2$ to $St_L/1.03 \approx St_L$. The approximations entering into our expression for V_{pg} are better, so no correction is applied. The final equation for V_{pp} is then

$$V_{pp}^2 = 1.6 V_g^2 \left[St_L - \frac{1}{St_L Re + Re^{1/2}} \right]. \qquad (23)$$

The results of equations (19) and (23) (the preferred and adjusted $n = 1$ forms), normalized by V_g, are shown in **figure 4** for the same three values of Re as in MMV, and in closeup form in **figure 5**.

As shown by MMV (their figure 2), and as seen previously in our figure 2, the falloff of V_{pp} is extremely steep for $St_\eta < 1$ (*i.e.* $St_L < Re^{-1/2}$ as shown in the scaling relations of section 1.6 above) because there is no more energy in faster eddies to provide relative velocities to such particles.

1.10 Simplification of analytically determined velocity expressions:

Equations (19) and (23) - for the preferred $n = 1$ case - are readily simplified in different limits of interest. It is simply shown by retaining leading terms that equation (19) for V_{pg}

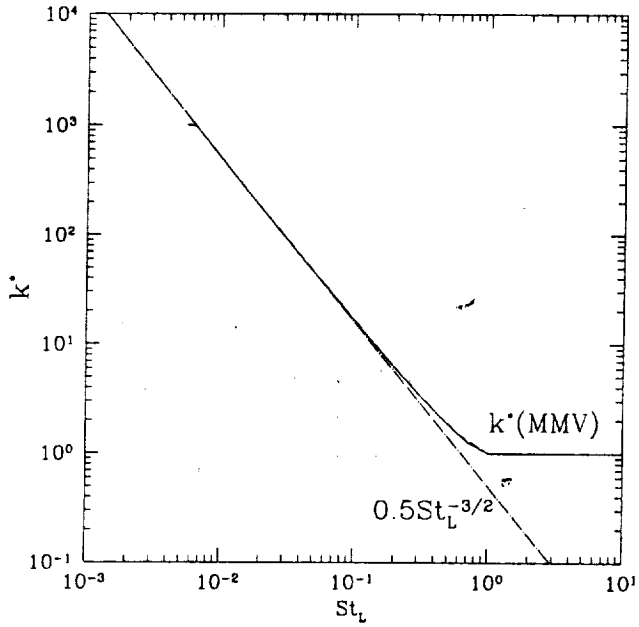

Figure 3: Correction of our approximation $k^* \approx St_L^{-3/2}$ by a factor of two (dash-dot line) which brings it into excellent agreement (in our range of validity $St_L < 0.1$) with the exact numerical solution for k^*, shown for $Re = 10^4$, 10^7, and 10^9, computed using the full VJMR/MMV expression. Only *very* close to $St_\eta = 1$ does our approximation deviate slightly; notice the tiny tail at $St_L = 6 \times 10^{-3}$, $k^* = 10^3$, which is the Kolmogorov scale for $Re = 10^4$.

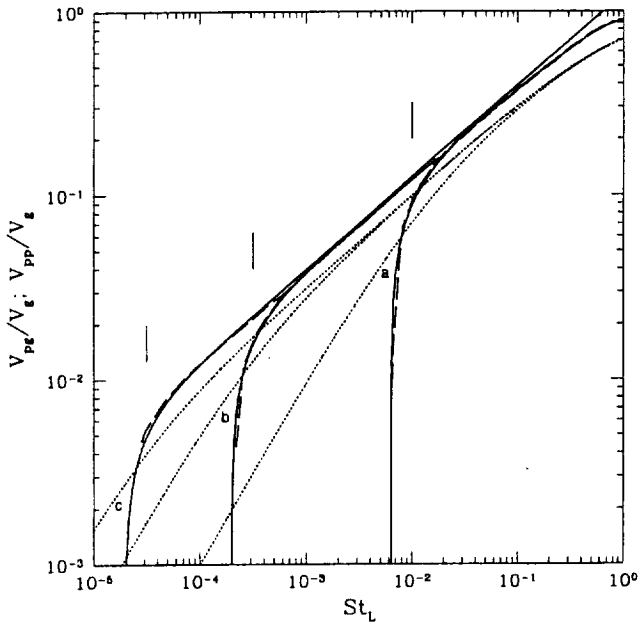

Figure 4: $V_{pg}(St_L)$ (dotted; equation 19) and $V_{pp}(St_L)$ (solid; equation 23) for $Re = 10^4$ (a), 10^7 (b), and 10^9 (c). The digitized results of MMV (their figure 5) for V_{pp}, for the same three values of Re, are shown by the dashed lines. Our V_{pp} expression is invalid for $St_L > 0.1$ or so (see text).

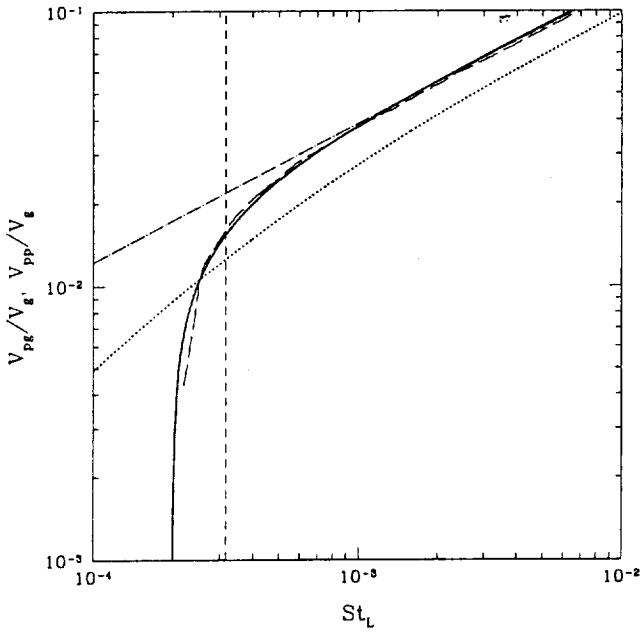

Figure 5: A closeup plot of V_{pg} (dotted), V_{pp} (solid), and the digitized MMV results (their figure 5) for V_{pp} (dashed, see Appendix) all for the $Re = 10^7$ case. The dash-dot line has slope 1/2. The vertical short dashed line indicates $St_\eta = 1$, where $St_L = Re^{-1/2}$; here, $V_{pg} \propto St_L^{0.75}$.

results in three separate regimes: $V_{pg} \approx V_g$ for $St_L > 1$, $V_{pg} \propto St_L^{1/2}$ for $Re^{-1/2} < St_L << 1$, and $V_{pg} \propto St_L Re^{1/4}$ for $St_L < Re^{-1/2}$. This is confirmed by inspection of figures 2 and 4. In the special case of $St_\eta = 1$, or $St_L = Re^{-1/2}$, equation (19) reduces directly to

$$V_{pg}(St_\eta = 1) = V_g \frac{Re^{-1/4}}{\sqrt{2}} = c\alpha^{1/4} \left(\frac{\nu}{4cH}\right)^{1/4}, \tag{24}$$

where we have substituted $V_g = c\alpha^{1/2}$ (Cuzzi *et al.* 2001). This Re-dependence, which also applies for $St_\eta < 1$ in general, quite naturally explains a result we obtained empirically from our numerical models over a range of Re much smaller than nebula values, namely that $V_{pg}/V_g \propto Re^{-1/4}$ (Cuzzi *et al.* 1998). By contrast, it is similarly shown from equation (20) that the St_L-dependence of V_{pg} for the older $n = 0$ case continues the $St_L^{1/2}$ dependence to arbitrarily small St_L.

These results are also consistent with arguments in Cuzzi *et al.* (1993, Appendix B; A. Dobrovolskis, personal communication). Expand and time-average the instantaneous quantity $< (V_p - V_g)^2 >$ to obtain $< V_{pg}V_{pg} >=< V_pV_p > + < V_gV_g > -2 < V_pV_g >$. Substituting from Cuzzi *et al.* (1993, equation B11) we find $< V_pV_p >=< V_pV_g >=< V_gV_g > /(1+St_L)$, leading to $V_{pg} = (St_L/(1+St_L))^{1/2} V_g$, which reaches the same limits as equation (19) *except* for particles with $t_s \leq t_\eta$, or $St_\eta \leq 1$, because the integral in its derivation (equation B11 of Cuzzi *et al.* 1993) extends to infinite eddy frequency.

Thus, unless $t_s \leq t_\eta$ ($St_L < Re^{-1/2}$), the particle-gas relative velocity in turbulence is generally proportional to $\sqrt{St_L}$ for small St_L. The steeper dependence of V_{pg} on St_L and St_η is restricted (in turbulence) to particles with $St_\eta \leq 1$. That is, evidence for a more nearly linear dependence of V_{pg} on r, if the environment was turbulent, would imply that the particles in question were $St_\eta \leq 1$ particles. This new result derives directly from the use of the $n = 1$ gas velocity autocorrelation function. The primary qualitative change is in the particle size dependence of V_{pg} for particles with $St_\eta \leq 1$. We address the significance of this in more detail in a forthcoming paper (Cuzzi 2002b).

Finally, using equation (23) for V_{pp}, we get

$$V_{pp}(St_\eta = 1) = \sqrt{0.8} V_g Re^{-1/4} = 1.26 V_{pg}, \tag{25}$$

where we used equation (24) for V_{pg}.

2 Comparison with numerical results

In this section we compare numerical results from our full 3D Lagrangian particle-gas model (Hogan *et al.* 1999) with full numerical calculations using our implementation of MMV (sections 1.8-1.9). We present particle velocities relative to the computational box (V_p), and relative to the local fluid velocity (V_{pg}), as obtained from our simulations. These velocities are defined as RMS spatial averages over all particles in a single snapshot, or $V = (< (V_x - < V_x >)^2 > + < (V_y - < V_y >)^2 > + < (V_z - < V_z >)^2 >)^{1/2}$, where V represents V_p or V_{pg} at the location of each particle, and $<>$ is the averaging operator $< ... >= \sum_{i=1}^{N_p}(...)/N_p$, where N_p is the number of particles in a single snapshot. Of course, $< V >$ is very close to zero for both these quantities since there is no mean flow in our simulations.

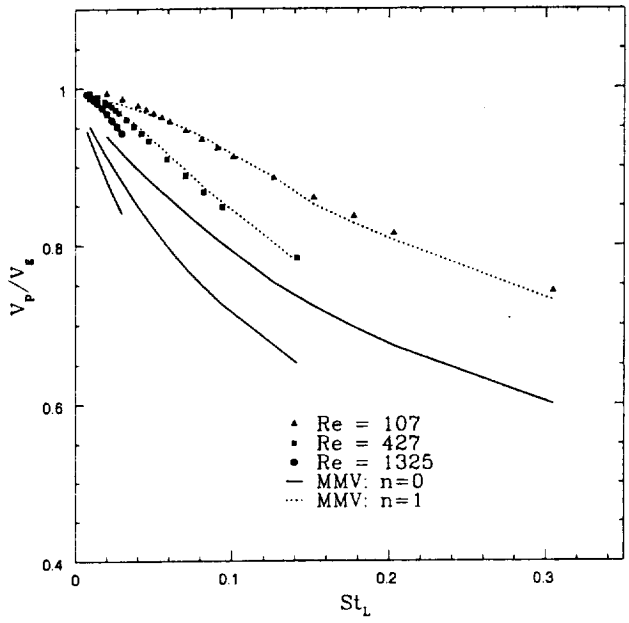

Figure 6: V_p *vs.* St_L obtained from our direct simulations compared with MMV predictions for models $n = 0$ (solid line) and $n = 1$ (dashed line). All velocities have been normalized by the RMS fluid velocity V_g. Results are shown for three different Re; the St_L values for each point are defined relative to a large eddy time based on energy dissipation[2], which varies with Re for our numerical calculations. When they are defined relative to a *constant* large eddy time, as are our analytical models and the MMV models shown in figure 2, points and models for all Re collapse onto the same curve as seen in figure 2. The $n = 1$ MMV prediction is clearly a better fit to the numerically simulated velocities, regardless of the choice of normalization timescale.

This spatial averaging approach is equivalent to the temporal averaging implicit in the MMV model, because of the ergodic principle that equates temporal and spatial averaging under suitable conditions. In our case, the conditions are satisified because our integral length scale L is small compared to the spatial period of the computational domain, for all Re.

The case of V_{pp} is more complicated, as the results depend on the proximity region chosen for "neighboring" particles. For the most useful comparisons with the predictions of MMV and VJMR, and with the expected uses of this quantity in mind, the region over which particle neighbors are selected should be as small as possible - less than η certainly - and here we run into sampling errors. Perhaps most important, the deviation of our model energy spectrum from a Kolmogorov spectrum is significant (*eg.* Squires and Eaton 1990), and V_{pp} is much more sensitive to the details of the high-spatial-frequency end of the energy spectrum than either V_p or V_{pg}. Since the main purpose of these calculations is to verify numerically the preference for the $n = 1$ autocorrelation function in an independent way from the direct comparison shown in figure 1, and because this case is already well made by the V_p and V_{pg} plots, we present no comparisons for V_{pp}.

Figures 6 - 9 show that the $n = 1$ autocorrelation function provides a much better

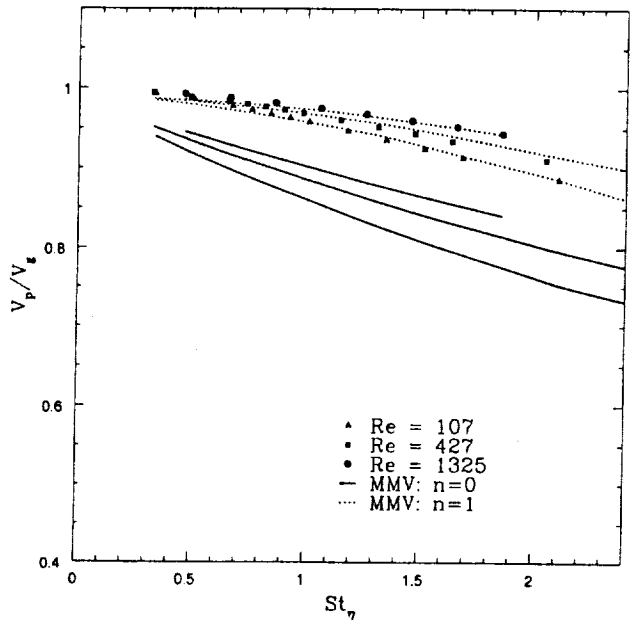

Figure 7: V_p, as in figure 6, but plotted against St_η.

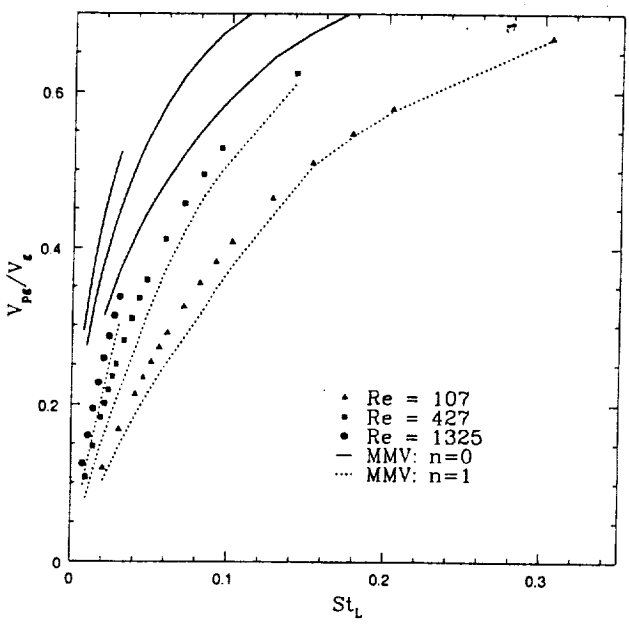

Figure 8: V_{pg} obtained from our direct simulations, compared with predictions of the MMV models with $n = 0$ (solid line) and $n = 1$ (dashed line) vs St_L. All curves have been normalized by the RMS fluid velocity V_g.

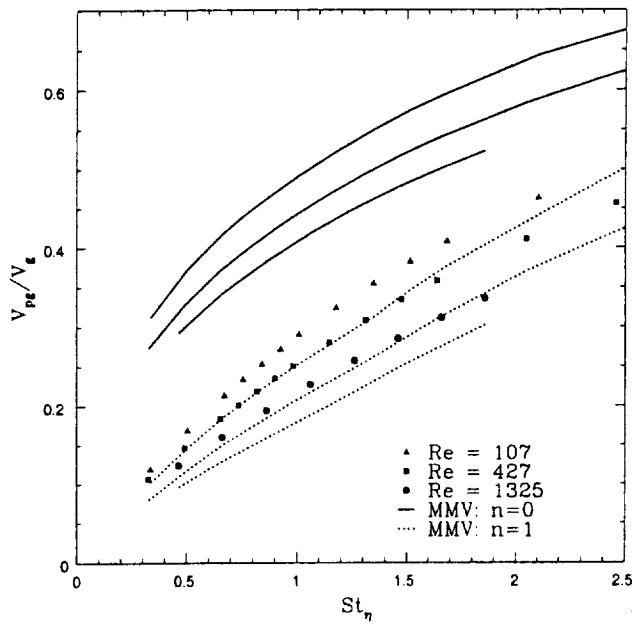

Figure 9: The same data shown in figure 8, but plotted against St_η.

fit to both V_p and V_{pg} than the $n = 0$ version. For V_{pg}, the fits of the MMV theory to our simulations are less perfect than for V_p. We can see several possible explanations for this. For instance, the mathematically simple form adopted for the $n = 1$ autocorrelation function is not a perfect fit to the actual numerically determined one (figure 1), by about the correct fractional amount. Also, we have emphasized that the correct velocity autocorrelation function to use is that *along a particle trajectory* (Meek and Jones 1973), and this function is actually somewhat size dependent even over the range $St_\eta \sim 1$ (see, *eg.*, Squires 1990, figure 4-23). Finally, because of the deviation of our turbulent kinetic energy spectrum from an inertial range, some of the definitions of eddy times used in the MMV theory might be inappropriate. It would not be surprising for V_{pg} to be more sensitive to these small deviations than V_p (compare figures 6 and 8, or 7 and 9). In spite of the small deviations in V_{pg}, the combination of the direct comparisons of the autocorrelation functions themselves (figure 1), and the comparison of the velocities derived using them (figures 6-9) makes it clear that the $n = 1$ autocorrelation function is the best choice.

3 Summary and conclusions

We present theoretical and numerical results which describe the turbulence-driven velocities of particles in the $St_L << 1$ size regime which might characterize chondrules and similar sized particles. We numerically verify the general approach of VJMR as modified by MMV, and verify in two different ways the intuitive preference of MMV for an $n = 1$ gas velocity autocorrelation function - at least along the trajectories of $St_\eta \approx 1$ particles. We find theoretically that the $n = 1$ autocorrelation function leads to a particle-gas relative velocity function that approaches linear dependence on particle size for particles in the $St_\eta \approx 1$

regime, and becomes and remains linear for arbitrarily small sizes. This is quite a different result than predicted by the original VJMR $n = 0$ expressions. We derive simple analytic expressions for V_p, V_{pg}, and V_{pp} (the latter, for comparable size particles only) for arbitrary levels of nebula intensity, as characterized by its Reynolds number Re or its corresponding "α". In a separate paper (Cuzzi 2002b) we will present some implications of these results for meteoritics.

Acknowledgements: We are grateful to Sandy Davis for helpful discussions on matters mathematical, to Robert Last for computational and graphics support, and to Wojtek Markiewicz for helpful discussions concerning MMV. We thank Ignacio Mosqueira, Steve Desch, Pat Cassen, and Tony Dobrovolskis for careful reading of the manuscript and helpful comments. This research was supported by Grants to JNC from the Planetary Geology and Geophysics Program and the Origins of Solar Systems Program.

Table I. List of symbols

Parameter	Definition
c	gas molecule thermal speed
C	particle concentration factor
$E(k)$	turbulent kinetic energy at wavenumber k
H	nebula vertical scale height
k	eddy wavenumber
k_L	wavenumber of largest eddy
k_η	wavenumber of Kolmogorov scale eddy
L	integral or largest scale in turbulent energy spectrum
r	particle radius
R	gas velocity autocorrelation function
Re	flow Reynolds number
St_L	Stokes number relative to largest eddy
St_η	Stokes number relative to Kolmogorov scale eddy
t_s	stopping time of particle due to gas drag
t_k	overturn time of eddy with wavenumber k
t_L	overturn time of largest eddy
t_η	overturn time of Kolmogorov scale eddy
V_g	gas turbulent velocity (large eddy)
V_p	particle random velocity in inertial space
V_{pg}	relative velocity between particles and gas
V_{pp}	relative velocity between particles
α	nebula viscosity parameter; $Re = \alpha c H/\nu$
ϵ	dissipation of turbulent kinetic energy
η	Kolmogorov scale
ν	molecular kinematic viscosity
ν_T	turbulent kinematic viscosity
ω	eddy temporal frequency
ρ_g	gas mass density
ρ_s	solid particle mass density

4 References

Adachi, I., C. Hayashi, and K. Nakazawa (1976) The gas drag effect on the elliptical motion of a solid body in the primordial solar nebula; Prog. Theor. Phys., 56, 1756-1771

Batchelor, G. K. (1948) Diffusion in a field of homogeneous turbulence II; The relative motion of particles; Proc. Camb. Phil. Soc. 48, 345-362

Boss, A. P. (1996) A concise guide to chondrule formation models; in "Chondrules and the Protoplanetary Disk", R. Hewins, R. Jones, and E. R. D. Scott, eds; Cambridge Univ. Press; pp 257-264

Brearley, A. J. and R. H. Jones (1998) Chondritic Meteorites, in "Planetary Materials", Revs. in Mineralogy, 36, Ch. 3; pgs 191ff.

Connolly, H. C and S. G. Love (1998) The formation of chondrules: petrologic tests of the shock wave model; Science, 280, 62-67

Csanady, G. T. (1963) Turbulent diffusion of heavy particles in the atmosphere; J. Atmos. Sci 14, 171-194

Cuzzi, J. N. (2002b) Blowing in the Wind: II. Diffusion and accretion of fine dust rims by small particles in a turbulent protoplanetary nebula; in preparation for Meteoritics and Planetary Science.

Cuzzi, J. N., A. R. Dobrovolskis, and J. M. Champney (1993) Particle-gas dynamics near the midplane of a protoplanetary nebula; Icarus, 106, 102-134

Cuzzi, J. N., A. R. Dobrovolskis, and R. C. Hogan (1996); Turbulence, Chondrules, and Planetesimals; in "Chondrules and the Protoplanetary Disk", R. Hewins, R. Jones, and E. R. D. Scott, eds; Cambridge Univ. Press; pp 35-44

Cuzzi, J. N., R. C. Hogan, J. M. Paque, and A. R. Dobrovolskis (2001) Size-selective concentration of chondrules and other small particles in protoplanetary nebula turbulence; Astrophys. J., 546, 496-508

Cuzzi, J. N., R. C. Hogan, J. M. Paque, and A. R. Dobrovolskis (1998) Chondrule rimming by sweepup of dust in the protoplanetary nebula : constraints on primary accretion; 29th LPSC

Elghobashi, S. E. (1991) Particle-laden turbulent flows: direct simulation and closure models; Applied Science Research, 48, 301-314

Grossman, J., A. E. Rubin, H. Nagahara, and E. A. King (1989) Properties of chondrules; in "Meteorites and the early solar system", J. F. Kerridge and M. S. Matthews, eds; Univ. of Arizona Press; p 619-659

Grossman, J. (1989) Formation of chondrules; in "Meteorites and the early solar system", J. F. Kerridge and M. S. Matthews, eds; Univ. of Arizona Press; p 680-696

Hinze, J. O. (1975) Turbulence, 2nd Ed. McGraw-Hill, New York, Chapter 5

Jones, R. H., T. Lee, H. C. Connolly Jr., S. G. Love, and H. Shang (2000) Formation of Chondrules and CAIs: Theory vs. Observation; in Protostars and Planets IV; V. Mannings, A. P. Boss, and S. S. Russell, eds, University of Arizona Press; p. 927

Markiewicz, W. J., H. Mizuno, and H. J. Völk (1991) Turbulence-induced relative velocity between two grains; Astron. Astrophys. 242, 286-289

Meek, C. C. and B. G. Jones (1973) Studies of the behavior of heavy particles in a turbulent fluid flow; J. Atm. Sciences, 30, 239-244

Metzler, K., and A. Bischoff (1996) Constraints on chondrite agglomeration from fine-grained chondrule rims; in "Chondrules and the Protoplanetary Disk", Cambridge University Press, Cambridge; R. Hewins, R. Jones, and E. R. D. Scott, eds

Morfill, G. E., R. H. Durisen, and G. W. Turner (1998) Note: An accretion rim constraint on chondrule formation theories; Icarus 134, 180-184

Paque, J., and J. N. Cuzzi (1997) Physical Characteristics of Chondrules and Rims, and Aerodynamic Sorting in the Solar Nebula; 28th LPSC Abstracts.

Scott, E. R. D., D. J. Barber, C. M. Alexander, R. Hutchison, and J. A. Peck (1989) Primitive material surviving in chondrules: Matrix; in "Meteorites and the early solar system", J. F. Kerridge and M. S. Matthews, eds; Univ. of Arizona Press; p 718-745

Squires, K. (1990) The interaction of particles with homogeneous turbulence; Thesis, Stanford University

Squires, K. and J. K. Eaton (1990) Particle response and turbulence modification in isotropic turbulence; Phys. Fluids A2, 1191-1203

Tennekes, H., and Lumley, J. L. (1972) A First Course in Turbulence, MIT Press, Cambridge Mass.

Völk, H. J., F. C. Jones, G. E. Morfill, and S. Röser (1978) Induced velocities of grains embedded in a turbulent gas; Moon and Planets, 19, 221-227

Völk, H. J., F. C. Jones, G. E. Morfill, and S. Röser (1980) Collisions between grains in a turbulent gas; Astron. Astrophys. 85, 316-325

Weidenschilling, S. J. (1977) Aerodynamics of solid bodies in the solar nebula; Mon. Not. Roy. Ast. Soc. 180, 57-70

Weidenschilling, S. J. (1980) Dust to planetesimals: settling and coagulation in the solar nebula; Icarus 44, 172-189

Whipple, F. (1973) Radial Pressure in the Solar Nebula as Affecting the Motions of Planetesimals; in Evolutionary and Physical Properties of Meteoroids, Proc. IAU Colloq. 13; C. L. Hemenway, P. M. Millman, and A. F. Cook, eds. NASA SP 319, p.355

Blowing in the Wind: I. Velocities of Chondrule-sized Particles in a Turbulent Protoplanetary Nebula

Jeffrey N. Cuzzi[1] and Robert C. Hogan[2]
[1] Space Science Division, Ames Research Center; cuzzi@cosmic.arc.nasa.gov
[2] Bay Area Environmental Research, inc.; hogan@cosmic.arc.nasa.gov
Submitted to Icarus, September 17, 2002

Abstract: Small but macroscopic particles - chondrules, higher temperature mineral inclusions, metal grains, and their like - dominate the fabric of primitive meteorites. The properties of these constituents, and their relationship to the fine dust grains which surround them, suggest that they led an extended existence in a gaseous protoplanetary nebula prior to their incorporation into their parent primitive bodies. In this paper we explore in some detail the velocities acquired by such particles in a turbulent nebula. We treat velocities in inertial space (relevant to diffusion), velocities relative to the gas and entrained microscopic dust (relevant to accretion of dust rims), and velocities relative to each other (relevant to collisions). We extend previous work by presenting explicit, closed-form solutions for the magnitude and size dependence of these velocities in this important particle size regime, and compare these expressions with new numerical calculations. The magnitude and size dependence of these velocities have immediate applications to chondrule and CAI rimming by fine dust, and to their diffusion in the nebula, which we explore separately.

1 Background

The fabric of the most primitive meteorites undoubtedly contains many clues as to their origin. While most chondrites are samples of surfaces that have been well worked over by impacts and stirring ("regolith breccias"), the dominance of chondrules and like-sized objects remains clear. How it came about that most chondrite parent bodies are so dominated by particles with such a well-defined range of physical, chemical, and petrographic properties remains one of the big puzzles of meteoritics. Since there are relatively few examples of anything larger than 0.1-10 mm size particles in most primitive planetesimals, the way such particles interact with the gaseous nebula is of prime importance.

Fe-Mg-Si-O mineral chondrules, which solidified from a melt, constitute 30-80% of primitive meteorites. There are a number of extant hypotheses for the formation of the chondrules. Most workers in the field believe that chondrules are formed by either localized or nebula scale energetic events operating on freely floating precursors of comparable mass, at some location or locations in the protoplanetary nebula. However, some still maintain they are made in or on primitive bodies, or in collisions between them. In a hybrid scenario, some suggest they are formed in shock waves generated by already-formed planetesimals, and thus that they are a secondary phenomenon to primary accretion of planetesimals. See *eg.* Grossman (1989), Grossman *et al.* (1989), Boss (1996), Connolly and Love (1999), and Jones *et al.* (2000) for reviews of hypotheses on this long-controversial and perennially fascinating subject.

Another meteorite constituent of great interest are the mineral grains called Ca-Al-rich refractory inclusions (CAIs) - so called because their constituent minerals condense out of nebula gas at a much higher temperature than do chondrules. These objects are widely believed to be direct nebula condensates, and have a complex subsequent thermal history which has some similarities to that of chondrules and some differences. There is some indication from radioisotope ages that CAIs might be $\sim 10^6$ years older than the chondrules, but this remains slightly controversial. They make up 1-10% of primitive meteorites depending on type, and their size distribution is broader than that of the chondrules. How these high-temperature minerals find themselves intimately mixed with lower-temperature minerals remains a puzzle.

It remains unresolved at this time whether the nebula gas was turbulent or laminar during the chondrule era. In previous papers, we have suggested that some of the observed properties of chondrules themselves - their typical size and size distribution - can be associated with, and easily explained by, the effects of weak nebula turbulence (Cuzzi et al 1996, 2001). Nevertheless, a consistent end-to-end scenario for *formation* of primitive bodies in this environment, and relying on these processes, is not yet in hand. In this paper, we focus on the velocity evolution of this specific class of particles in a weakly turbulent nebula as a step towards developing a more complete scenario that operates to produce primitive bodies in a similar way across a variety of environments. The velocity evolution is critical for our understanding of several important aspects of chondrules and chondrites: (a) the radial distribution and redistribution or transport of chondrules and/or CAIs, once formed, before their accumulation into parent bodies; (b) The presence of fine grained rims on chondrules, CAIs, and other coarse particles in primitive chondrites (Metzler and Bischoff 1996, Brearley and Jones 1998); and (c) collision rates and velocities between chondrule-sized particles. The main goal of this paper is to provide a theoretical framework within which we can better understand mm-to-cm-size particle evolution in general. We accomplish this in sections 1 (analytical theory) and 2 (supporting numerical calculations). In another paper we apply these results to diffusion and dust rimming (Cuzzi 2002b).

1.1 Particle Velocities in Turbulence

Astrophysical modeling of the basic physics of particle behavior in fluid flows, laminar or turbulent, tends to begin and end with the classic papers by Whipple (1973), Adachi *et al.* (1976), Weidenschilling (1977, 1980), and Völk *et al.* (1980, henceforth VJMR; also Völk *et al.* 1978), with important recent updates by Markiewicz *et al.* (1991; henceforth MMV). In the fluid dynamics literature, however, the study of particle motions in fluid flows has both a long history, and a robust ongoing presence. This history is nicely summarized by Meek and Jones (1973). More recent work in the fluids literature is noted in various relevant places below. VJMR first developed a useful formalism for calculating the dispersion velocities V_p (relative to inertial space) and collision velocities V_{pp} (relative to each other) of particles in a turbulent nebula. They circumvented the thorny problem of "essential nonlinearity" (*cf.* Meek and Jones 1973) by translating clever physical insights into mathematics and adopting a velocity autocorrelation function approach, which we discuss in more detail below. While it serves an important internal role in their solutions, neither VJMR nor MMV say much about the relative velocity between particles and gas, V_{pg}. Yet, V_{pg} is the determinant quantity for

accretion of rims of fine dust grains by small, macroscopic objects (Paque and Cuzzi 1997, Cuzzi et al 1998, Morfill *et al.* 1998). Our goal in this paper is to quantify V_p, V_{pg}, and V_{pp} for such particles in a way that extends and focusses the formulation of VJMR and MMV, and which allows insights to be gained into the history of chondrules and like-sized particles in the protoplanetary nebula.

In this paper, we determine velocities of all three kinds - V_p, V_{pg}, and V_{pp} - with emphasis on particles having stopping times t_s comparable to the overturn time t_η of Kolmogorov scale eddies. Particles in this size regime have behavior more complex than tiny "dust" grains, which are essentially trapped to the gas flow on all scales. In particular, particles with $t_s = t_\eta$ are subject to "preferential concentration" by large factors in turbulence, and based on some of its apparent fingerprints in the meteorite record, we have suggested a link between this process, chondrules, and primary accretion. Specifically, we refer to the fact that the *typical size* and the *shape of the size distribution* of chondrules are readily explained by turbulent concentration (Cuzzi et al 1996, 2001). In a parallel paper (Cuzzi 2002b) we explore the possibility that the functional form of V_{pg} might reveal another fingerprint of turbulent concentration, and that turbulence might help us understand the puzzling mix of CAIs and chondrules in the same meteorites.

Particles are aerodynamically classified by their Stokes number St, the ratio of their stopping time t_s to the overturn time of some characteristic eddy. We will make use of Stokes numbers defined relative to two different eddy overturn timescales: the Stokes number relative to the largest, or integral scale eddy time t_L: $St_L = t_s/t_L$, and that defined relative to the smallest, or Kolmogorov scale eddy time t_η: $St_\eta = t_s/t_\eta$. The overturn time of the largest scale eddy t_L is generally regarded as the local orbit period. Preferentially concentrated particles (chondrules, we believe) have $St_\eta = 1$ and $St_L << 1$. For these particles, which are smaller than the gas molecular mean free path, the stopping time $t_s = r\rho_s/c\rho_g$, where r is particle radius, ρ_s is particle material density, c is the nebula sound speed, and ρ_g is the nebula gas density (Weidenschilling 1977). That is, t_s and thus both St_L and St_η are *linearly proportional to particle radius.*

1.2 Previous work; the autocorrelation function

We briefly review and simplify the notation of VJMR and MMV. VJMR assumed a fully developed inertial range of turbulence with some largest, or integral scale L and zero smallest scale. MMV also adopted the Kolmogorov energy spectrum (as shall we) but correctly pointed out that turbulence ceases for scales smaller than the Kolmogorov or inner scale η. Especially for small particles in the chondrule-and-CAI size range, MMV point out that this has important implications for V_p and V_{pp}, and we will show that the implications are important for V_{pg} as well. In a Kolmogorov spectrum, an inertial range of turbulent gas kinetic energy extends from the largest or integral scale $l = L$ to the smallest or Kolmogorov scale $l = \eta$. Following VJMR, we work in the spatial frequency regime, where $k(l) = 2\pi/l$ and $E(k) = E_L(k/k_L)^{-5/3}$ for the Kolmogorov spectrum (note our $E(k)$ is a true energy, and is half of VJMR's $P(k)$). Then $v(k) = (2kE(k))^{1/2}$ and $t(k) = 1/(kv(k)) = t_L(k/k_L)^{-2/3}$. As did MMV, we assume $E(k) = 0$ for $k > k_\eta$ (no turbulent energy at scales smaller than the Kolmogorov scale). The mean square turbulent (fluctuating) gas velocity is V_g; thus the typical turbulent kinetic energy per unit gas mass is $V_g^2/2$, providing the normalization

criterion:

$$\int_{k_L}^{k_\eta} E(k)dk = V_g^2/2 = \int_{k_L}^{k_\eta} E_L(k/k_L)^{-5/3}dk = \frac{3}{2}E_L k_L. \quad (1)$$

The turbulent gas motions induce fluctuating velocities in the particle population, leading to diffusion (V_p), mutual collisions (V_{pp}), and motion relative to the local gas (V_{pg}).

VJMR derive V_p formally by a backwards time integration of the instantaneous acceleration (their equations 5 and 6):

$$V_p(t) = t_s^{-1} \int_0^t \exp\left(-(t-t')/t_s\right) V_g(t')dt' \quad (2)$$

where $V_g(t')$ represents the fluctuating gas velocity history along a particle trajectory (formally unknown at this point). They proceed by approximating $V_g(t')$ as an integral over all (independently acting) spatial frequencies k with eddy timescales t_k, and approximate the contributions as coming from two classes of eddies: "class 1" eddies, with overturn times long enough ($t_k > t_s$) that particles are always in equilibrium within them, and are primarily just advected by their (temporally fluctuating) motions, and "class 3" eddies with overturn times too short ($t_k < t_s$) for the particle to come to equilibrium as it passes through them. Intermediate, or what might be "class 2" eddies are not treated separately, but simply absorbed into the classes on either side. Different simplifications are allowed for each class. The boundary between eddy classes 1 and 3 is k^*, where $t_{k*} = t_s$. VJMR show that the class 3 (small, fast) eddies are negligible for velocity components V_p and V_{pg}, but dominate the contributions to V_{pp}. We will make use of these results below.

VJMR first obtain the product $< V_p(t)V_p(t) >=< V_p^2 >$ by integrating backwards over two separate time histories. They introduce the gas velocity autocorrelation function for gas velocities (in their equation 16) $R(t,t';k) = \exp\left(-|t-t'|/t_k\right)$. While they don't make the distinction, the autocorrelation function to be used in this way is properly that determined *along a particle trajectory* (Batchelor 1948, Hinze 1975, Squires and Eaton 1990, Elghobashi 1991), and is thus a function of t_s in general. However, for $St_L << 1$, and at this stage of our knowledge, this distinction is not significant (Squires 1990).

Subsequently, MMV suggested a more general, even if *ad hoc*, functional form for $R(t,t';k)$:

$$R(t,t';k) = \left(1 + \frac{|t-t'|}{t_k}\right)^n e^{(-|t-t'|/t_k)}, \quad (3)$$

with $n = 0$ or 1. They note that the $n = 1$ case has more plausible physical behavior (zero slope) near $t = t'$ than the $n = 0$ (pure exponential) form assumed by VJMR.

1.2.1 New results regarding the form of the autocorrelation function, and the value of n:

The selection of $n = (0, 1)$ determines the form of the fluid velocity autocorrelation function $R(t,t';k)$. Squires (1990) measured this function directly in his direct numerical simulations of turbulence, by following fluid motions along the trajectories of a number of particles with different St_L. In **figure 1** we compare the results of Squires (1990) with the predictions based on the $n = 0$ and $n = 1$ expressions of MMV for $R(t,t';k)$. Note that, since MMV

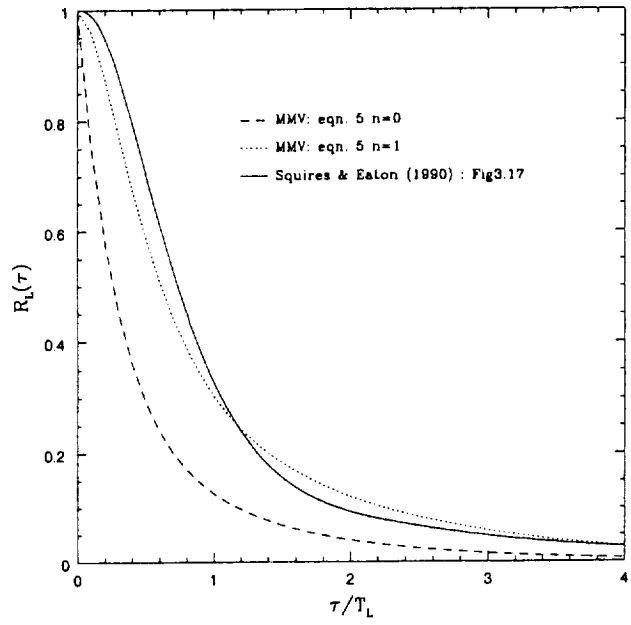

Figure 1: Autocorrelation function for gas velocities along the trajectory of a $St_\eta = 1$ particle, as computed directly from our simulations (dotted) and from the simulations of Squires (1990), and as calculated using the $n = 0$ and $n = 1$ models of MMV. Here, $\tau = t - t'$ and is normalized by the large eddy turnover time T_L. The $n = 1$ model is clearly the better choice.

express their autocorrelation function as a function of k, it must be integrated over an energy spectrum to compare with the numerical results of Squires (1990). Because Squires (1990) only calculated a 1-D autocorrelation function (*ie.*, using only one velocity component), we integrated the $R(t, t'; k)$ of MMV over a 1D energy spectrum (essentially, one-third of the total $E(k)$) (see also Squires and Eaton 1991). It is clear from figure 1 that $n = 1$ is the better choice. This has important implications, primarily for V_{pg} and V_{pp}. In section 2, we directly compare V_p and V_{pg} calculated in full 3D turbulence using the two alternate autocorrelation functions, and again reach the same conclusion.

1.3 Particle random velocities relative to inertial space

After some algebra, VJMR derive an expression (their equation 18) for the mean square particle fluctuating velocity V_p, of which we need only the large, slow (class 1) eddy contribution since the small eddy contribution is negligible for $St_\eta = 1$ particles (we will henceforth drop the $<>$ notation on V_p, V_g, V_{pg}, and V_{pp}, and will merely recall that all are statistical expectation values based on extensive temporal or spatial averaging). Because of our emphasis on particles with $St_\eta = 1$, we also replace the upper limit of VJMR's class 1 integral (k^*) with the Kolmogorov scale k_η. This simplification is, in fact, actually fairly good over the entire range of $St_L << 1$, *precisely because* the contribution of eddies on smaller scales than k^* (the class 3 eddies) is negligible. That is, the upper limit can be extended from k^* to k_η *in general* for mathematical simplicity without incurring significant error. Mathematically,

the upper limit could even be extended to infinity (*eg.*, Völk *et al.* 1980), but the important role of the Reynolds number and of the Kolmogorov scale is then lost. Thus,

$$V_p^2 \approx 2 \int_{k_L}^{k_\eta} E(k) \frac{t_k}{t_k + t_s} dk. \tag{4}$$

Similarly, the generalized MMV expression for V_p^2 (their equation 6) can be simplified to

$$V_p^2 \approx 2 \int_{k_L}^{k_\eta} E(k) \left(1 - \left(\frac{t_s}{t_k + t_s}\right)^{n+1}\right) dk = 2 \int_{k_L}^{k_\eta} E(k) \left(1 - \left(\frac{1}{1 + t_k/t_s}\right)^{n+1}\right) dk \tag{5}$$

for the particle size regime of interest here. As did VJMR, MMV note that the second integral of their equation (6) - the class 3 eddy contribution - is negligible for small particles, so we retain only the first integral of their equation (6). We again simplify the upper limit of integration in the remaining integral for the nominal $St_\eta \approx 1$ case where $k^* \approx k_\eta >> k_L$. We validate this by comparing our results with those of MMV (section 1.7).

The result for V_p^2 was plotted, but not stated explicitly, by VJMR and MMV (figure 1 in both papers), and explicitly derived by Cuzzi *et al.* (1993; Appendix B): $V_p^2 = V_g^2/(1+St_L)$. It is simple to see why $V_p^2 \approx V_g^2$ in the limit $St_L << 1$ and certainly for $St_\eta \approx 1$, since $t_s << t_k$ in equations (4) or (5) for nearly all k and overwhelmingly all $E(k)$. This limit is appropriate for chondrule-and-CAI-sized particles even in the presence of their small vertical settling velocity - they diffuse nearly as well as a gas molecule, and do not "settle to the midplane" in even a very weakly turbulent nebula (Dubrulle *et al.* 1995, Cuzzi *et al.* 1996). The implications are discussed in section 3. However, V_p^2 and V_g^2 are not *exactly* equal, resulting in a small, but very important, relative energy of motion V_{pg}^2, giving the velocity with which particles move through the gas and encounter tiny (micron-sized) dust grains.

1.4 Particle velocities relative to the gas

The average relative velocity magnitude between a particle and the turbulent gas is V_{pg}. VJMR make use only of the spatial frequency components of this quantity, which they refer to as $V_{rel}(k)$ (their equation 15). Practically speaking, however, a particle will instantaneously sense all eddy contributions as one V_{pg}; we obtain this by merely integrating VJMR equation (15) over k. Considering only the part of the expression relevant for $St_\eta \approx 1$ (that for $k^* > k_L$), neglecting any systematic velocity, and again letting $k^* \approx k_\eta >> k_L$, the second integral vanishes and we obtain

$$V_{pg}^2 \approx 2 \int_{k_L}^{k_\eta} E(k) \left(\frac{t_s}{t_k + t_s}\right) dk. \tag{6}$$

For this $n = 0$ case treated by VJMR, it can be easily verified using equations (4) and (6) that

$$V_{pg}^2 + V_p^2 = 2 \int_{k_L}^{k_\eta} E(k) dk = V_g^2. \tag{7}$$

However, this useful result is true independent of n. It may also be obtained by Fourier transform solution of the forcing equations in temporal frequency (ω) space, where the

energy spectrum of gas velocity fluctuations $E_g(\omega)$, particle velocity fluctuations $E_p(\omega)$, and relative velocity fluctuations $E_{pg}(\omega)$ are related by

$$E_p(\omega) = E_g(\omega)/(1 + t_s^2\omega^2) \quad \text{and} \quad E_{pg}(\omega) = t_s^2\omega^2 E_p(\omega). \tag{8}$$

This approach can be traced to Csanady (1963); it is also described by Hinze (1975, chapter 5), Meek and Jones (1973), and Squires (1990, sections 4.2 and 4.5.1)). The E_p solution was also derived in this way by Cuzzi *et al.* (1993, Appendix B). It is also clear then that $E_{pg}(\omega) + E_p(\omega) = E_g(\omega)$, essentially the same result as equation (7) above. Finally, we have directly verified equation (7) in our numerical simulations.

Using this general relationship, we can extend the results of MMV to obtain V_{pg}^2 for their more generalized gas velocity autocorrelation functions (they only present results for V_p^2). That is, using equations (1) and (5),

$$V_{pg}^2 = V_g^2 - V_p^2 = 2\int_{k_L}^{k_\eta} E(k)(\frac{t_s}{t_s + t_k})^{n+1} dk = 2\int_{k_L}^{k_\eta} E(k)\left(\frac{1}{1 + t_k/t_s}\right)^{n+1} dk. \tag{9}$$

We will use equations (5) and (9), with assumed inertial range expressions for $E(k)$, to derive analytical expressions for V_p and V_{pg} of hypothetically "chondrule-like" (*ie.*, $St_\eta \approx 1$) particles as functions of their size and the turbulent Reynolds number.

1.5 Relative velocities between particles of similar sizes

Expressions for V_{pp} (VJMR Appendix C and equation 19; MMV equations 7 and 8) are more cumbersome, but respond nicely to certain simplifying assumptions. The full expression for V_{pp} for two particles of equal size is (changing notation slightly from MMV equation 9, and allowing for a finite Kolmogorov scale):

$$V_{pp}^2 = 4\int_{k^*}^{k_\eta} E(k)\left(1 - \frac{t_s}{t_s + t_k}\right)\left[g(\chi) + \frac{nt_s h(\chi)}{t_s + t_k}\right] dk, \tag{10}$$

where $g(\chi) = \tan^{-1}(\chi)/\chi$ and $h(\chi) = 1/(1 + \chi^2)$. The parameter χ of VJMR and MMV is small in our regime of interest:

$$\chi = \frac{V_{rel}(k)t_s(kt_k)}{t_s + t_k} = \frac{V_{rel}(k)t_s}{v(k)(t_s + t_k)} \approx \frac{V_{rel}(k)}{2v(k)} < 1, \tag{11}$$

since in the very limited range of k over which the integral is done, $t_s \approx t_k$.[1] In fact $\chi << 1$ over most of the integral where $t_s << t_k$, so the functions $g(\chi)$ and $h(\chi)$ are ≈ 1 or perhaps as small as a fraction of order unity; thus

$$V_{pp}^2 \approx 4\int_{k^*}^{k_\eta} E(k)\left[1 - \left(\frac{t_s}{t_s + t_k}\right)^{n+1}\right] dk = 4\int_{k^*}^{k_\eta} E(k)\left[1 - \left(\frac{1}{1 + t_k/t_s}\right)^{n+1}\right] dk. \tag{12}$$

The integrand is identical to that for V_p^2, but the integral has different limits which make it clear that only the eddies faster than t_s can perturb identical particles into having incoherent relative velocities.

[1] In the above equation, the mathematical generalization of V_{pg} by VJMR and MMV to its $k-$th components $V_{rel}(k)$ momentarily reappears. However, it is true in general, at any spatial frequency, that the particle-gas relative velocity is less than, or at most equal to, the gas velocity itself.

1.6 Scaling relations

Recall that for the gas,

$$t_k = l(k)/v(k) = (L/V_g)(k/k_L)^{-2/3} = t_L(k/k_L)^{-2/3} \tag{13}$$

(Cuzzi *et al.* 2001). In equation (13) we have made the usual identification of V_g with the largest scale eddy L. For the particles,

$$\frac{t_s}{t_L} = St_L = (k_s/k_L)^{-2/3} \tag{14}$$

and

$$\frac{t_s}{t_k} = (k/k_s)^{2/3} = \frac{t_s}{t_L}(k/k_L)^{2/3} = St_L(k/k_L)^{2/3}, \tag{15}$$

Note that if we restrict our attention to particles *with* $St_\eta = t_s/t_\eta \approx 1$, then their Stokes number referred to the *integral* scale automatically becomes

$$St_L = t_s/t_L = t_\eta/t_L = (k_\eta/k_L)^{-2/3} = (Re^{3/4})^{-2/3} = Re^{-1/2}. \tag{16}$$

The last substitution of $(k_\eta/k_L) = Re^{3/4}$, where $Re = LV_g/\nu$ is the flow Reynolds number, with ν being the molecular kinematic viscosity, is a direct consequence of the definitions of the Kolmogorov scale, the energy dissipation rate, and the Reynolds number (Tennekes and Lumley 1972). This relation can be obtained without any reference at all to the Kolmogorov spectrum but merely using scaling arguments relating to t_L and t_η.[2] Re is related to astrophysical "α"-models of the protoplanetary nebula by $Re = \alpha cH/\nu$ with c = sound speed and H = nebula vertical scale height (Cuzzi *et al.* 2001).

1.7 Final expressions for V_{pg} and V_{pp}

Substituting the scaling relations from above for t_s/t_k, equation (9) for V_{pg} becomes

$$V_{pg}^2 = 2\int_{k_L}^{k_\eta} E(k)\left(\frac{1}{1+t_k/t_s}\right)^{n+1} dk = 2\int_{k_L}^{k_\eta} E(k)\left(\frac{St_L}{St_L+(k/k_L)^{-2/3}}\right)^{n+1} dk. \tag{17}$$

We use the normalization (equation 1) to write $E(k) = (V_g^2/3k_L)(k/k_L)^{-5/3}$, and change integration variable to $x = k/k_L$, leaving

$$V_{pg}^2 = \frac{2V_g^2}{3}\int_1^{Re^{3/4}} \left(\frac{St_L}{St_L+x^{-2/3}}\right)^{n+1} x^{-5/3}dx. \tag{18}$$

where in the upper limit we have substituted $k_\eta/k_L = Re^{3/4}$ from the scaling relations. Closed form solutions for equation (18) can be obtained for $n = 0$ or 1. For example, for $n = 1$ the result of the integral is

$$V_{pg}^2 = V_g^2\left[\frac{St_L}{1+St_Lx^{2/3}}\right]_{Re^{3/4}}^1 = V_g^2\left[\frac{St_L^2(Re^{1/2}-1)}{(St_L+1)(St_LRe^{1/2}+1)}\right]. \tag{19}$$

[2]Let the energy dissipation rate be ϵ. Then $\epsilon = V_g^2/t_L = V_g^3/L$ where the first expression defines t_L and the last expression defines L. Also $t_\eta = (\nu/\epsilon)^{1/2}$ and $\eta = (\nu^3/\epsilon)^{1/4}$. Solving gives $t_L/t_\eta = Re^{1/2}$ and $\eta/L = Re^{3/4}$.

For $n = 0$ the result of the integral is:

$$V_{pg}^2 = V_g^2 \left[St_L \ln \left(\frac{Re^{1/2}(1 + St_L)}{Re^{1/2} St_L + 1} \right) \right]. \tag{20}$$

These results make it quite easy to predict both the magnitude and the St_η dependence of V_{pg} for arbitrary nebula turbulent intensity.

We solve equation (12) for V_{pp} in a similar fashion to the solution for V_{pg} above, to obtain for $n = 1$:

$$V_{pp}^2 = \frac{4V_g^2}{3} \int_{k(t_s)/k_L}^{k_\eta/k_L} \left(\frac{2St_L x^{-7/3} + x^{-9/3}}{St_L^2 + 2St_L x^{-2/3} + x^{-4/3}} \right) dx. \tag{21}$$

As before, the upper integration limit is $k_\eta/k_L = Re^{3/4}$. For the lower limit, $k^*/k_L = k(t_s)/k_L = (t_s/t_L)^{-3/2} = St_L^{-3/2}$ from the scaling relations. The closed form analytic solution of this integral is:

$$V_{pp}^2 = 2V_g^2 \left[\frac{x^{-2/3}}{1 + St_L x^{2/3}} \right]_{Re^{3/4}}^{St_L^{-3/2}} = 2V_g^2 \left[\frac{St_L}{2} - \frac{1}{St_L Re + Re^{1/2}} \right]. \tag{22}$$

The $n = 0$ form of the solution is somewhat less useful, and we note it without expanding it as it will not be used further.

$$V_{pp}^2 = 2V_g^2 \left[St_L \ln \left(\frac{1 + St_L x^{2/3}}{x^{2/3}} \right) - \frac{1}{x^{2/3}} \right]_{St_L^{-3/2}}^{Re^{3/4}}.$$

1.8 Detailed comparisons with the models of Markiewicz *et al.*

In addition to developing the analytical expressions discussed and applied in the paper, we also developed a detailed numerical model following the prescriptions of MMV exactly (but with a generalized turbulent energy spectrum). This was needed both to evaluate their theoretical approach in the context of our numerical simulations of turbulence (section 2), which have a non-Kolmogorov spectrum and low Reynolds number compared to nebula applications, and to assess the validity of our analytical approximations. The numerical model of MMV is no longer in active use (W. Markiewicz, personal communication 2002), so we digitized their V_{pp} results (their figure 5) to facilitate comparisons. As seen in **figure 4**, our full numerical model for V_{pp} (solid curves) agrees very well with their results for V_{pp} (long dashed curves). In figure 2 we also show our results for V_{pg}, not presented by VJMR or MMV, as obtained by integrating MMV equation 4 over all spatial frequencies. Note that we, and MMV, both use the appropriate form of $R(t, t'; k)$ (*ie.*, that for the correct choice of n; section 1.2) for these calculations.

The most striking feature of the results, first noted by MMV, is that V_{pp} very quickly falls to zero for particles with $St_\eta < 1$ (*i.e.* $St_L < Re^{-1/2}$, as shown in the scaling relations of section 1.6 above) because there is no more energy in faster eddies to provide relative velocities to such particles. This does not happen to V_{pg}, because eddies on all scales contribute. Also note that V_p and V_{pp} decrease for *large* particles ($St_L > 1$), as fewer eddies can effectively

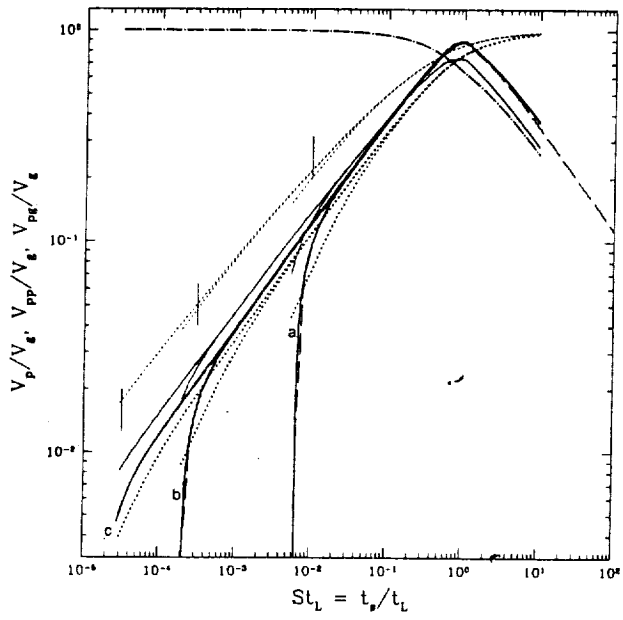

Figure 2: Comparison of our numerical version of the full MMV model for $n = 0$ (light curves) and $n = 1$ (heavy curves), along with digitized results for V_{pp} from MMV (dashed curves, their figure 5, for $n = 1$). Three different Re are shown: (a) 10^4, (b) 10^7, and (c) 10^9. The dash-dot curves are for V_p, which has the same shape for all three Re. V_{pg} is shown in the two sets of dotted curves and V_{pp} in the two sets of solid curves. Note that the $n = 0$ values of V_{pg} (light dotted curves) are considerably (3-4 times) higher than the preferred $n = 1$ values (heavy dotted curves), *and* the St_L-dependence of V_{pg}, for $n = 0$, never gets much above 0.5, whereas for $n = 1$ a linear dependence is seen for $St_L < Re^{-1/2}$. As in figures 4 and 5, vertical hash marks correspond to $St_L = Re^{-1/2}$ for the three values of Re.

couple to particles with such long stopping times. Naturally, V_{pg} simply approaches V_g for these large particles.

Upon comparing our original analytical results (equations 19 and 22) with our full numerical model and the MMV results, we found some small quantitative discrepancies at the order unity level, as might be expected. The responsible approximations were easily identified. First, we approximated the boundary between class 1 and class 3 eddies by $t_s = t(k^*)$ rather than the more complete equation 9 of VJMR and equation 4 of MMV, which obtains the relevant eddy frequency in the moving frame of the particle and involves $V_{rel}(k)$. Comparison of the two criteria revealed that, to a very good approximation, the criterion $t_s = t(k^*)$ gives a value of k^* that is too large by a factor close to 2 (**figure 3**). So, after this "calibration", we merely decrease the lower limit of integration in our equation (22) by a factor of 2. Second, even after this correction, our values of V_{pp} are about 20% high. This is easily ascribed to our approximation that $g(\chi)$ and $h(\chi)$ are equal to unity throughout the entire range of k; in fact, they are tens of percent smaller than unity over some part of this range, depending on the value of St_L. Empirically, this is corrected by multiplying our analytical expression for V_{pp} by a constant factor of 0.8. With these two simple adjustments, each correcting a known oversimplification, our analytical expression for V_{pp} achieves very good good agreement with the MMV results, and with our own full numerical model, over the relevant range of $St_L \leq 0.1$ or so. There appears to be no reason to make such refinements to our analytical expression for V_{pg} (equatión 19), because our approximations are better justified and the agreement with MMV acceptable.

1.9 Numerical refinements to the model

With insights gained from comparison of our numerical and analytical models, we have made two small adjustments to equation (22) for V_{pp} which correct for two of our approximations. Equation (22) is multiplied by a factor of 0.8, and the upper integration limit ($St_L^{-3/2}$) is divided by two, so the first term in the final expression changes from $St_L/2$ to $St_L/1.03 \approx St_L$. The approximations entering into our expression for V_{pg} are better, so no correction is applied. The final equation for V_{pp} is then

$$V_{pp}^2 = 1.6 V_g^2 \left[St_L - \frac{1}{St_L Re + Re^{1/2}} \right]. \tag{23}$$

The results of equations (19) and (23) (the preferred and adjusted $n = 1$ forms), normalized by V_g, are shown in **figure 4** for the same three values of Re as in MMV, and in closeup form in **figure 5**.

As shown by MMV (their figure 2), and as seen previously in our figure 2, the falloff of V_{pp} is extremely steep for $St_\eta < 1$ (*i.e.* $St_L < Re^{-1/2}$ as shown in the scaling relations of section 1.6 above) because there is no more energy in faster eddies to provide relative velocities to such particles.

1.10 Simplification of analytically determined velocity expressions:

Equations (19) and (23) - for the preferred $n = 1$ case - are readily simplified in different limits of interest. It is simply shown by retaining leading terms that equation (19) for V_{pg}

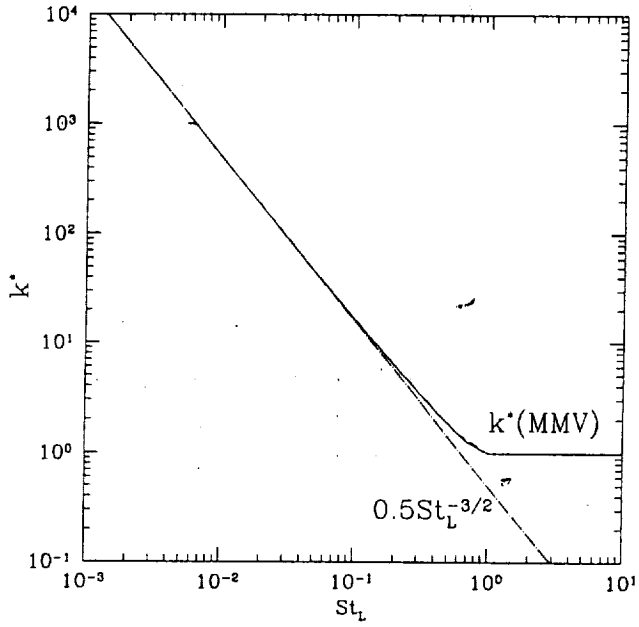

Figure 3: Correction of our approximation $k^* \approx St_L^{-3/2}$ by a factor of two (dash-dot line) which brings it into excellent agreement (in our range of validity $St_L < 0.1$) with the exact numerical solution for k^*, shown for $Re = 10^4$, 10^7, and 10^9, computed using the full VJMR/MMV expression. Only *very* close to $St_\eta = 1$ does our approximation deviate slightly; notice the tiny tail at $St_L = 6 \times 10^{-3}$, $k^* = 10^3$, which is the Kolmogorov scale for $Re = 10^4$.

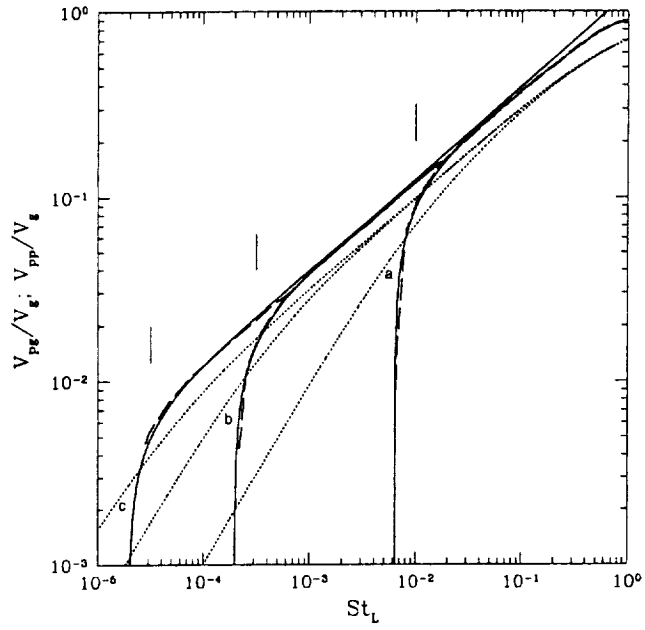

Figure 4: $V_{pg}(St_L)$ (dotted; equation 19) and $V_{pp}(St_L)$ (solid; equation 23) for $Re = 10^4$ (a), 10^7 (b), and 10^9 (c). The digitized results of MMV (their figure 5) for V_{pp}, for the same three values of Re, are shown by the dashed lines. Our V_{pp} expression is invalid for $St_L > 0.1$ or so (see text).

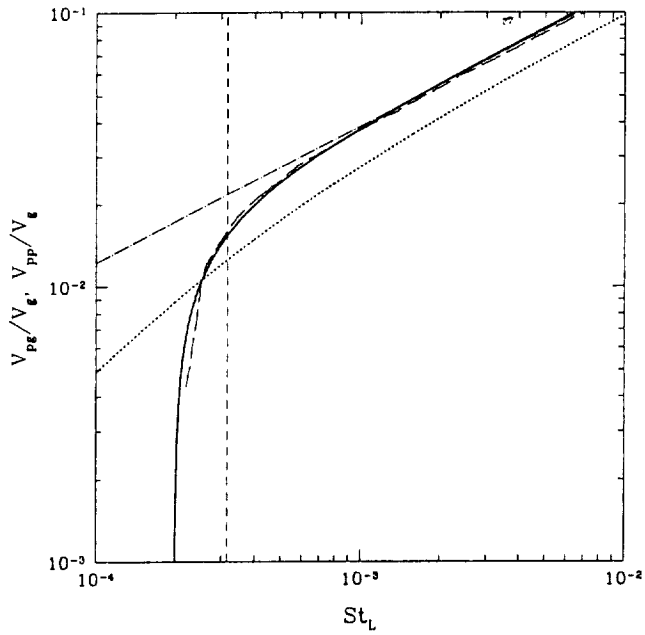

Figure 5: A closeup plot of V_{pg} (dotted), V_{pp} (solid), and the digitized MMV results (their figure 5) for V_{pp} (dashed, see Appendix) all for the $Re = 10^7$ case. The dash-dot line has slope 1/2. The vertical short dashed line indicates $St_\eta = 1$, where $St_L = Re^{-1/2}$; here, $V_{pg} \propto St_L^{0.75}$.

results in three separate regimes: $V_{pg} \approx V_g$ for $St_L > 1$, $V_{pg} \propto St_L^{1/2}$ for $Re^{-1/2} < St_L << 1$, and $V_{pg} \propto St_L Re^{1/4}$ for $St_L < Re^{-1/2}$. This is confirmed by inspection of figures 2 and 4. In the special case of $St_\eta = 1$, or $St_L = Re^{-1/2}$, equation (19) reduces directly to

$$V_{pg}(St_\eta = 1) = V_g \frac{Re^{-1/4}}{\sqrt{2}} = c\alpha^{1/4} \left(\frac{\nu}{4cH}\right)^{1/4}, \tag{24}$$

where we have substituted $V_g = c\alpha^{1/2}$ (Cuzzi *et al.* 2001). This Re-dependence, which also applies for $St_\eta < 1$ in general, quite naturally explains a result we obtained empirically from our numerical models over a range of Re much smaller than nebula values, namely that $V_{pg}/V_g \propto Re^{-1/4}$ (Cuzzi *et al.* 1998). By contrast, it is similarly shown from equation (20) that the St_L-dependence of V_{pg} for the older $n = 0$ case continues the $St_L^{1/2}$ dependence to arbitrarily small St_L.

These results are also consistent with arguments in Cuzzi *et al.* (1993, Appendix B; A. Dobrovolskis, personal communication). Expand and time-average the instantaneous quantity $< (V_p - V_g)^2 >$ to obtain $< V_{pg}V_{pg} >=< V_pV_p > + < V_gV_g > -2 < V_pV_g >$. Substituting from Cuzzi *et al.* (1993, equation B11) we find $< V_pV_p >=< V_pV_g >=< V_gV_g > /(1+St_L)$, leading to $V_{pg} = (St_L/(1+St_L))^{1/2} V_g$, which reaches the same limits as equation (19) *except* for particles with $t_s \leq t_\eta$, or $St_\eta \leq 1$, because the integral in its derivation (equation B11 of Cuzzi *et al.* 1993) extends to infinite eddy frequency.

Thus, unless $t_s \leq t_\eta$ ($St_L < Re^{-1/2}$), the particle-gas relative velocity in turbulence is generally proportional to $\sqrt{St_L}$ for small St_L. The steeper dependence of V_{pg} on St_L and St_η is restricted (in turbulence) to particles with $St_\eta \leq 1$. That is, evidence for a more nearly linear dependence of V_{pg} on r, if the environment was turbulent, would imply that the particles in question were $St_\eta \leq 1$ particles. This new result derives directly from the use of the $n = 1$ gas velocity autocorrelation function. The primary qualitative change is in the particle size dependence of V_{pg} for particles with $St_\eta \leq 1$. We address the significance of this in more detail in a forthcoming paper (Cuzzi 2002b).

Finally, using equation (23) for V_{pp}, we get

$$V_{pp}(St_\eta = 1) = \sqrt{0.8} V_g Re^{-1/4} = 1.26 V_{pg}, \tag{25}$$

where we used equation (24) for V_{pg}.

2 Comparison with numerical results

In this section we compare numerical results from our full 3D Lagrangian particle-gas model (Hogan *et al.* 1999) with full numerical calculations using our implementation of MMV (sections 1.8-1.9). We present particle velocities relative to the computational box (V_p), and relative to the local fluid velocity (V_{pg}), as obtained from our simulations. These velocities are defined as RMS spatial averages over all particles in a single snapshot, or $V = (< (V_x - < V_x >)^2 > + < (V_y - < V_y >)^2 > + < (V_z - < V_z >)^2 >)^{1/2}$, where V represents V_p or V_{pg} at the location of each particle, and $<>$ is the averaging operator $< ... >= \sum_{i=1}^{N_p}(...)/N_p$, where N_p is the number of particles in a single snapshot. Of course, $< V >$ is very close to zero for both these quantities since there is no mean flow in our simulations.

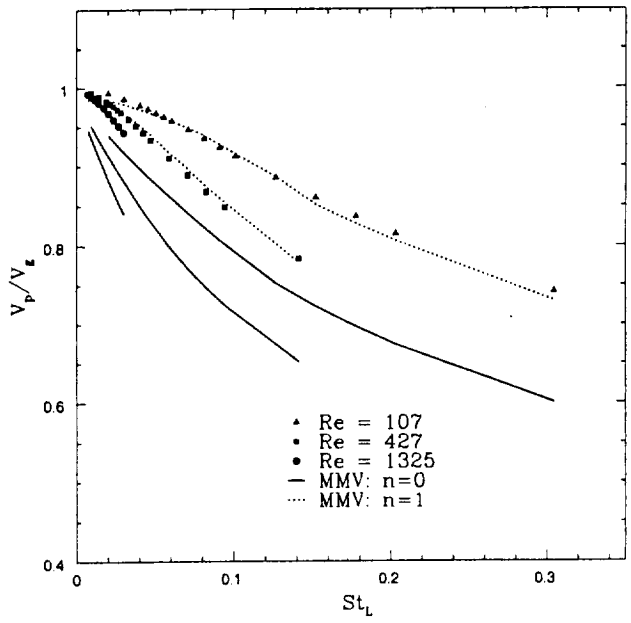

Figure 6: V_p *vs.* St_L obtained from our direct simulations compared with MMV predictions for models $n = 0$ (solid line) and $n = 1$ (dashed line). All velocities have been normalized by the RMS fluid velocity V_g. Results are shown for three different Re; the St_L values for each point are defined relative to a large eddy time based on energy dissipation[2], which varies with Re for our numerical calculations. When they are defined relative to a *constant* large eddy time, as are our analytical models and the MMV models shown in figure 2, points and models for all Re collapse onto the same curve as seen in figure 2. The $n = 1$ MMV prediction is clearly a better fit to the numerically simulated velocities, regardless of the choice of normalization timescale.

This spatial averaging approach is equivalent to the temporal averaging implicit in the MMV model, because of the ergodic principle that equates temporal and spatial averaging under suitable conditions. In our case, the conditions are satisified because our integral length scale L is small compared to the spatial period of the computational domain, for all Re.

The case of V_{pp} is more complicated, as the results depend on the proximity region chosen for "neighboring" particles. For the most useful comparisons with the predictions of MMV and VJMR, and with the expected uses of this quantity in mind, the region over which particle neighbors are selected should be as small as possible - less than η certainly - and here we run into sampling errors. Perhaps most important, the deviation of our model energy spectrum from a Kolmogorov spectrum is significant (*eg.* Squires and Eaton 1990), and V_{pp} is much more sensitive to the details of the high-spatial-frequency end of the energy spectrum than either V_p or V_{pg}. Since the main purpose of these calculations is to verify numerically the preference for the $n = 1$ autocorrelation function in an independent way from the direct comparison shown in figure 1, and because this case is already well made by the V_p and V_{pg} plots, we present no comparisons for V_{pp}.

Figures 6 - 9 show that the $n = 1$ autocorrelation function provides a much better

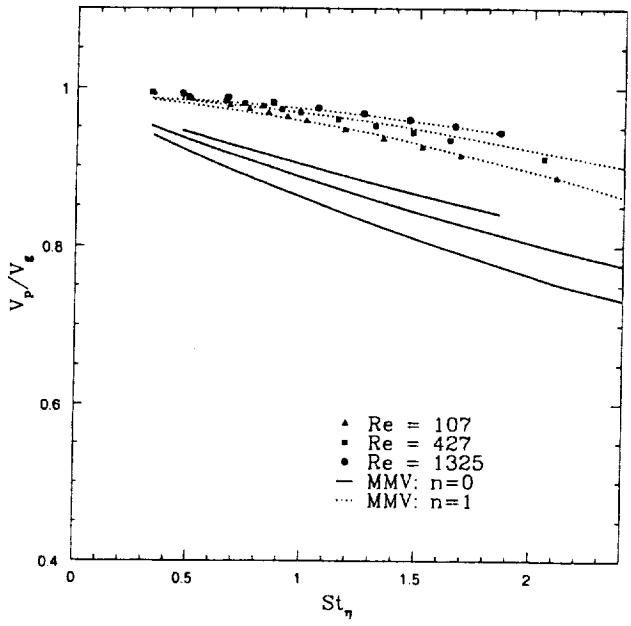

Figure 7: V_p, as in figure 6, but plotted against St_η.

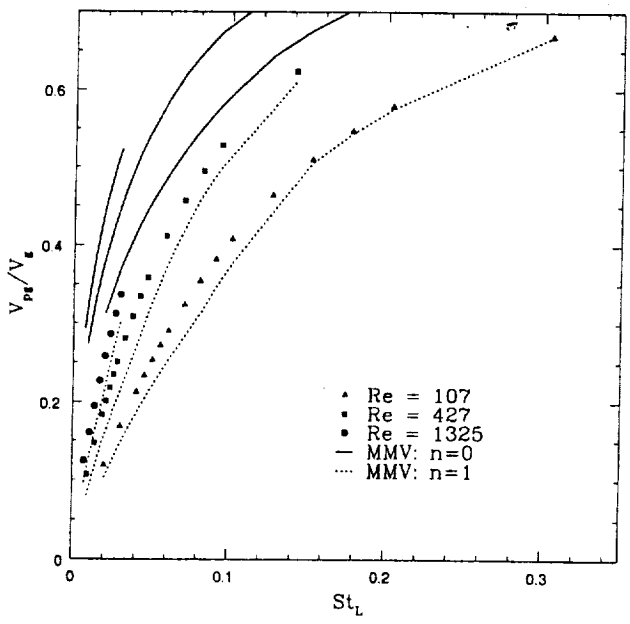

Figure 8: V_{pg} obtained from our direct simulations, compared with predictions of the MMV models with $n = 0$ (solid line) and $n = 1$ (dashed line) vs St_L. All curves have been normalized by the RMS fluid velocity V_g.

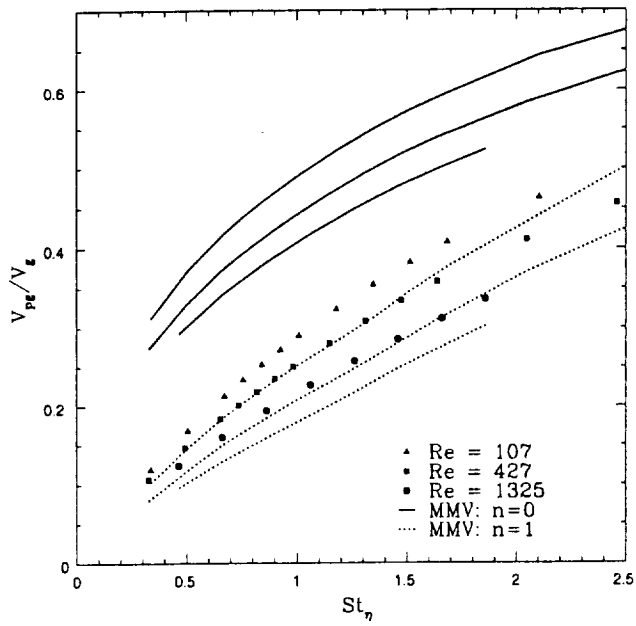

Figure 9: The same data shown in figure 8, but plotted against St_η.

fit to both V_p and V_{pg} than the $n = 0$ version. For V_{pg}, the fits of the MMV theory to our simulations are less perfect than for V_p. We can see several possible explanations for this. For instance, the mathematically simple form adopted for the $n = 1$ autocorrelation function is not a perfect fit to the actual numerically determined one (figure 1), by about the correct fractional amount. Also, we have emphasized that the correct velocity autocorrelation function to use is that *along a particle trajectory* (Meek and Jones 1973), and this function is actually somewhat size dependent even over the range $St_\eta \sim 1$ (see, *eg.*, Squires 1990, figure 4-23). Finally, because of the deviation of our turbulent kinetic energy spectrum from an inertial range, some of the definitions of eddy times used in the MMV theory might be inappropriate. It would not be surprising for V_{pg} to be more sensitive to these small deviations than V_p (compare figures 6 and 8, or 7 and 9). In spite of the small deviations in V_{pg}, the combination of the direct comparisons of the autocorrelation functions themselves (figure 1), and the comparison of the velocities derived using them (figures 6-9) makes it clear that the $n = 1$ autocorrelation function is the best choice.

3 Summary and conclusions

We present theoretical and numerical results which describe the turbulence-driven velocities of particles in the $St_L << 1$ size regime which might characterize chondrules and similar sized particles. We numerically verify the general approach of VJMR as modified by MMV, and verify in two different ways the intuitive preference of MMV for an $n = 1$ gas velocity autocorrelation function - at least along the trajectories of $St_\eta \approx 1$ particles. We find theoretically that the $n = 1$ autocorrelation function leads to a particle-gas relative velocity function that approaches linear dependence on particle size for particles in the $St_\eta \approx 1$

regime, and becomes and remains linear for arbitrarily small sizes. This is quite a different result than predicted by the original VJMR $n = 0$ expressions. We derive simple analytic expressions for V_p, V_{pg}, and V_{pp} (the latter, for comparable size particles only) for arbitrary levels of nebula intensity, as characterized by its Reynolds number Re or its corresponding "α". In a separate paper (Cuzzi 2002b) we will present some implications of these results for meteoritics.

Acknowledgements: We are grateful to Sandy Davis for helpful discussions on matters mathematical, to Robert Last for computational and graphics support, and to Wojtek Markiewicz for helpful discussions concerning MMV. We thank Ignacio Mosqueira, Steve Desch, Pat Cassen, and Tony Dobrovolskis for careful reading of the manuscript and helpful comments. This research was supported by Grants to JNC from the Planetary Geology and Geophysics Program and the Origins of Solar Systems Program.

Table I. List of symbols

Parameter	Definition
c	gas molecule thermal speed
C	particle concentration factor
$E(k)$	turbulent kinetic energy at wavenumber k
H	nebula vertical scale height
k	eddy wavenumber
k_L	wavenumber of largest eddy
k_η	wavenumber of Kolmogorov scale eddy
L	integral or largest scale in turbulent energy spectrum
r	particle radius
R	gas velocity autocorrelation function
Re	flow Reynolds number
St_L	Stokes number relative to largest eddy
St_η	Stokes number relative to Kolmogorov scale eddy
t_s	stopping time of particle due to gas drag
t_k	overturn time of eddy with wavenumber k
t_L	overturn time of largest eddy
t_η	overturn time of Kolmogorov scale eddy
V_g	gas turbulent velocity (large eddy)
V_p	particle random velocity in inertial space
V_{pg}	relative velocity between particles and gas
V_{pp}	relative velocity between particles
α	nebula viscosity parameter; $Re = \alpha cH/\nu$
ϵ	dissipation of turbulent kinetic energy
η	Kolmogorov scale
ν	molecular kinematic viscosity
ν_T	turbulent kinematic viscosity
ω	eddy temporal frequency
ρ_g	gas mass density
ρ_s	solid particle mass density

4 References

Adachi, I., C. Hayashi, and K. Nakazawa (1976) The gas drag effect on the elliptical motion of a solid body in the primordial solar nebula; Prog. Theor. Phys., 56, 1756-1771

Batchelor, G. K. (1948) Diffusion in a field of homogeneous turbulence II; The relative motion of particles; Proc. Camb. Phil. Soc. 48, 345-362

Boss, A. P. (1996) A concise guide to chondrule formation models; in "Chondrules and the Protoplanetary Disk", R. Hewins, R. Jones, and E. R. D. Scott, eds; Cambridge Univ. Press; pp 257-264

Brearley, A. J. and R. H. Jones (1998) Chondritic Meteorites, in "Planetary Materials", Revs. in Mineralogy, 36, Ch. 3; pgs 191ff.

Connolly, H. C and S. G. Love (1998) The formation of chondrules: petrologic tests of the shock wave model; Science, 280, 62-67

Csanady, G. T. (1963) Turbulent diffusion of heavy particles in the atmosphere; J. Atmos. Sci 14, 171-194

Cuzzi, J. N. (2002b) Blowing in the Wind: II. Diffusion and accretion of fine dust rims by small particles in a turbulent protoplanetary nebula; in preparation for Meteoritics and Planetary Science.

Cuzzi, J. N., A. R. Dobrovolskis, and J. M. Champney (1993) Particle-gas dynamics near the midplane of a protoplanetary nebula; Icarus, 106, 102-134

Cuzzi, J. N., A. R. Dobrovolskis, and R. C. Hogan (1996); Turbulence, Chondrules, and Planetesimals; in "Chondrules and the Protoplanetary Disk", R. Hewins, R. Jones, and E. R. D. Scott, eds; Cambridge Univ. Press; pp 35-44

Cuzzi, J. N., R. C. Hogan, J. M. Paque, and A. R. Dobrovolskis (2001) Size-selective concentration of chondrules and other small particles in protoplanetary nebula turbulence; Astrophys. J., 546, 496-508

Cuzzi, J. N., R. C. Hogan, J. M. Paque, and A. R. Dobrovolskis (1998) Chondrule rimming by sweepup of dust in the protoplanetary nebula : constraints on primary accretion; 29th LPSC

Elghobashi, S. E. (1991) Particle-laden turbulent flows: direct simulation and closure models; Applied Science Research, 48, 301-314

Grossman, J., A. E. Rubin, H. Nagahara, and E. A. King (1989) Properties of chondrules; in "Meteorites and the early solar system", J. F. Kerridge and M. S. Matthews, eds; Univ. of Arizona Press; p 619-659

Grossman, J. (1989) Formation of chondrules; in "Meteorites and the early solar system", J. F. Kerridge and M. S. Matthews, eds; Univ. of Arizona Press; p 680-696

Hinze, J. O. (1975) Turbulence, 2nd Ed. McGraw-Hill, New York, Chapter 5

Jones, R. H., T. Lee, H. C. Connolly Jr., S. G. Love, and H. Shang (2000) Formation of Chondrules and CAIs: Theory vs. Observation; in Protostars and Planets IV; V. Mannings, A. P. Boss, and S. S. Russell, eds, University of Arizona Press; p. 927

Markiewicz, W. J., H. Mizuno, and H. J. Völk (1991) Turbulence-induced relative velocity between two grains; Astron. Astrophys. 242, 286-289

Meek, C. C. and B. G. Jones (1973) Studies of the behavior of heavy particles in a turbulent fluid flow; J. Atm. Sciences, 30, 239-244

Metzler, K., and A. Bischoff (1996) Constraints on chondrite agglomeration from fine-grained chondrule rims; in "Chondrules and the Protoplanetary Disk", Cambridge University Press, Cambridge; R. Hewins, R. Jones, and E. R. D. Scott, eds

Morfill, G. E., R. H. Durisen, and G. W. Turner (1998) Note: An accretion rim constraint on chondrule formation theories; Icarus 134, 180-184

Paque, J., and J. N. Cuzzi (1997) Physical Characteristics of Chondrules and Rims, and Aerodynamic Sorting in the Solar Nebula; 28th LPSC Abstracts.

Scott, E. R. D., D. J. Barber, C. M. Alexander, R. Hutchison, and J. A. Peck (1989) Primitive material surviving in chondrules: Matrix; in "Meteorites and the early solar system", J. F. Kerridge and M. S. Matthews, eds; Univ. of Arizona Press; p 718-745

Squires, K. (1990) The interaction of particles with homogeneous turbulence; Thesis, Stanford University

Squires, K. and J. K. Eaton (1990) Particle response and turbulence modification in isotropic turbulence; Phys. Fluids A2, 1191-1203

Tennekes, H., and Lumley, J. L. (1972) A First Course in Turbulence, MIT Press, Cambridge Mass.

Völk, H. J., F. C. Jones, G. E. Morfill, and S. Röser (1978) Induced velocities of grains embedded in a turbulent gas; Moon and Planets, 19, 221-227

Völk, H. J., F. C. Jones, G. E. Morfill, and S. Röser (1980) Collisions between grains in a turbulent gas; Astron. Astrophys. 85, 316-325

Weidenschilling, S. J. (1977) Aerodynamics of solid bodies in the solar nebula; Mon. Not. Roy. Ast. Soc. 180, 57-70

Weidenschilling, S. J. (1980) Dust to planetesimals: settling and coagulation in the solar nebula; Icarus 44, 172-189

Whipple, F. (1973) Radial Pressure in the Solar Nebula as Affecting the Motions of Planetesimals; in Evolutionary and Physical Properties of Meteoroids, Proc. IAU Colloq. 13; C. L. Hemenway, P. M. Millman, and A. F. Cook, eds. NASA SP 319, p.355